LPTENS-97/2
hep-th@xxx/9706145
June 1997

The BPS Spectra and Superconformal Points in Massive $N = 2$ Supersymmetric QCD

Adel Bilal

and

Frank Ferrari

CNRS - Laboratoire de Physique Théorique de l'École Normale Supérieure[⋆]
24 rue Lhomond, 75231 Paris Cedex 05, France
adel.bilal@physique.ens.fr, frank.ferrari@physique.ens.fr

ABSTRACT

We present a detailed study of the analytic structure, BPS spectra and superconformal points of the $N = 2$ susy SU(2) gauge theories with $N_f = 1, 2, 3$ massive quark hypermultiplets. We compute the curves of marginal stability with the help of the explicit solutions for the low energy effective actions in terms of standard elliptic functions. We show that only a few of these curves are relevant. As a generic example, the case of $N_f = 2$ with two equal bare masses is studied in depth. We determine the precise existence domains for each BPS state, and show how they are compatible with the RG flows. At the superconformal point, where two singularities coincide, we prove that (for $N_f = 2$) the massless spectrum consists of *four* distinct BPS states and is S-invariant. This is due to the monodromy around the superconformal point being S, providing strong evidence for exact S-duality of the SCFT. For all N_f, we compute the slopes ω of the β-functions at the fixed point couplings and show that they are related to the anomalous dimensions α of $u = \langle \mathrm{tr}\, \phi^2 \rangle$ by $\omega = 2(\alpha - 1)$.

⋆ Unité Propre de Recherche 701 du CNRS, associée à l'École Normale Supérieure et à l'Université Paris-Sud.

1. Introduction

Many new insights into the physics of strongly coupled gauge theories have been obtained by the study of $N = 2$ supersymmetric Yang-Mills theories [1,2]. Two particularly interesting phenomena that occur in these four-dimensional theories are the discontinuities of the BPS spectra [3,4,5] on the Coulomb branch and the occurrence of superconformal points that are believed to lead to non-trivial interacting 4D superconformal field theories (SCFT) [6,7].

In the present paper we study the probably simplest case where both phenomena occur: the SU(2) theories with massive quark hypermultiplets. The discontinuities of the BPS spectra and the properties at the superconformal points are of course closely related and our study of the first will shed important new light on the second, and vice versa.

The main ingredients in the study of the $N = 2$ gauge theories are duality and holomorphicity of the low-energy effective action. The properties of the latter are encoded in a (hyper) elliptic curve which also determines the abelian charges of the theory. The BPS states constitute a particularly important sector of the Hilbert space: all perturbative and known solitonic states are BPS states. Their masses are determined by the abelian charges and hence by the (hyper) elliptic curve. Quite surprisingly, the latter also allows us to extract and determine the existence domains of the BPS states on the Coulomb branch of the moduli space $\mathcal{M}$. Indeed, BPS states generically are stable, except on real codimension one hypersurfaces in $\mathcal{M}$ (i.e. real dimension one curves for SU(2)). These instability hypersurfaces are determined in terms of the abelian charges and the quantum numbers of the BPS state.

For the SU(2) theories without or with N_f *massless* quark hypermultiplets ($N_f = 1, 2, 3$) there only is a *single* instability curve on $\mathcal{M} \simeq \mathbf{C}$. This curve is closed and goes through the singular points on $\mathcal{M}$. The BPS spectra are different inside and outside the curve [3,4,5]. We found that in the region outside the curve, part of which is the semiclassical domain, all semiclassically expected states exist. These are: the dyons $(n_e, n_m) = (2n, 1)$ for $N_f = 0$, the quarks $(1, 0)$ and the dyons $(n, 1)$ for $N_f = 1, 2, 3$, with in addition dyons $(2n + 1, 2)$ of magnetic charge two for $N_f = 3$. There also is the W-boson $(2, 0)$ for all N_f. In the region inside the instability curve, which always is a region of strong coupling, there only exist the states that are responsible for the singularities, i.e. the states that can become massless. For $N_f = 0$ e.g., these are the dyons $(0, 1)$ and $(-2\epsilon, 1)$ while for $N_f = 2$ these are $(0, 1)$ and $(-\epsilon, 1)$. Here ϵ equals $+1$ in the upper and -1 in the lower half plane. Almost all BPS states disappear when crossing the curve from outside to inside: they "decay" into the only two (or three) existing states. In particular, there is no W-boson inside the curve, although the gauge symmetry is always broken $\mathrm{SU}(2) \to \mathrm{U}(1)$.

The determination of these BPS spectra was relatively easy since there was only one instability curve. The generic situation of SU(n) is much more complicated: each BPS state has its own family of possible instability hypersurfaces. At first sight it seems hopeless to study this general case by the methods of [3,4]. However, a similar situation already occurs in the SU(2) theories with *massive* hypermultiplets. This is the case we study in the present paper. It will turn out that among the multitude of possible decay curves only a relatively small subset is relevant, and one obtains a very clear picture of the existence domains of the various BPS

states. We are quite confident that this structure can be exploited to also determine the exact BPS spectra at any point on the Coulomb branch of the SU(n) moduli space.

Another feature, absent in the massless SU(2) theories, but present for the higher SU(n) theories or the SU(2) theories with massive hypermultiplets, is the existence of superconformal points. These can occur at special points on the Coulomb branch in the SU(n) theories where singular lines intersect, or in the massive SU(2) theories at special values of the masses when singular points collide. In any case, at a superconformal point two or more mutually non-local BPS states simultaneously become massless [6]. To study these points, it will turn out to be most fruitful to view them as resulting from such a coincidence of individual singularities.

In this paper, we will discuss the BPS spectra of the SU(2) theories with $N_f = 1, 2, 3$ massive quark hypermultiplets, and present an in depth study of the $N_f = 2$ theory with equal bare masses. This latter case is sufficiently generic to exhibit all interesting new phenomena. We determine the precise existence domains for each BPS state and confirm these results by many additional consistency checks. We will also see how the whole set of decay curves and BPS spectra very consistently behaves under the RG flow from one N_f theory to another. A subtlety present in the massive theories is related to the abelian s_i-charges ($i = 1, \dots N_f$) [8] which we need to determine for all BPS states. Some indications on the BPS spectra of the massive theories were already obtained in [9] within the geodesics approach from string theory [10]. However, it only provided some partial and pointwise information on $\mathcal{M}$.[⋆]

The analytic structure and the corresponding monodromies are fundamental for our study. As we follow the various RG flows, we reach various superconformal points where the monodromies are given by the products of the individual monodromies of the coinciding singularities. Such a composite monodromy $M_{\rm sc}$ is quite special, acting e.g. as S-duality relating mutually non-local states as monopoles and quarks. We argue that it should be an exact quantum symmetry of the massless BPS sector and thus of the superconformal field theories. This monodromy (completely) characterises the SCFT allowing us to compute scaling dimensions. We show that the SCFT is determined in terms of a single integer $k = 1, 2$ or 3 characteristic of $M_{\rm sc}$. This is reminiscent to the study of the relevant deformations of the singular curves $y^2 = x^3$ in [7]. As we follow the RG flow further, the singularities separate again but the analytic structure is changed, providing us with an explanation of how the nature of certain singularities can change from being due to a massless quark at weak coupling to being due to a massless dyon at strong coupling.

Let us outline the organisation of the present paper and some of our results: first, in Section 2, we recall the elliptic curves for the massive $N_f = 1, 2, 3$ theories and discuss the quantum numbers of the BPS states associated with the singularities and how they change under the various RG flows one can study. This brings us naturally to a discussion of the superconformal points and how they are classified by an integer $k = 1, 2, 3$ through their monodromies. Then,

⋆ Where comparable, both results agree. Although there is a slight discrepancy with the published version of [9], after a first circulation of the present paper, the authors of [9] have informed us that this is only due to some error when writing up their paper but that they actually agree with our results, see Section 4 below.

we compute the basic functions $a_D(u)$ and $a(u)$, which are the period integrals of a certain meromorphic one-form, in terms of standard elliptic integrals in a form immediately suited for numerical computations. Technical details are postponed to the appendices. Similar results were also obtained independently and published recently in [11,12]. In Section 3, we discuss general features of the BPS spectra and the decay curves for all the massive $N_f = 1, 2, 3$ theories. In particular, we discuss the maximal possible set of BPS states compatible with the RG flow.

Section 4 then is an in depth study of the $N_f = 2$ theory with two equal bare masses m. There exists a superconformal point when $m = \frac{\Lambda_2}{2}$, and we discuss separately the cases $m < \frac{\Lambda_2}{2}$ and $m > \frac{\Lambda_2}{2}$. We find that all curves and existence domains of BPS states have perfectly smooth RG flows. In particular, the crossover from small mass ($m < \frac{\Lambda_2}{2}$) to large mass ($m > \frac{\Lambda_2}{2}$) is perfectly smooth, except, in a certain sense, at the superconformal point u_* itself. Also, as m becomes very large, in a basis $\tilde{a}_D,\ \tilde{a}$ that flows to the $a_D^{(N_f=0)},\ a^{(N_f=0)}$ only the states with $\tilde{s} = 0$ survive under the RG flow $m \to \infty$ to the pure gauge theory $N_f = 0$. At a given fixed point $u \in \mathcal{M}$, almost all $\tilde{s} \neq 0$ dyons disappear, already at finite m, because they are "hit" by their corresponding decay curves that move outwards (to large $|u|$) as m is increased. Among the $\tilde{s} \neq 0$ states only the quarks and some special dyons exist for all finite m, but as $m \to \infty$, their BPS masses diverge and thus they simply drop out of the spectrum for this reason. On the other hand, the different $\tilde{s} = 0$ states decay on one and the same curve which flows to the curve of the $N_f = 0$ theory. Thus we are able to see the flow to the $N_f = 0$ spectra in full detail. For each case, $m < \frac{\Lambda_2}{2}$ and $m > \frac{\Lambda_2}{2}$, we first discuss the general picture, which is then established by considering each class of BPS states separately.

The BPS spectra for $N_f = 2$, $m = \frac{\Lambda_2}{2}$ are then simply obtained as the limit of those for either $m > \frac{\Lambda_2}{2}$ or $m < \frac{\Lambda_2}{2}$. Nothing changes dramatically for $m = \frac{\Lambda_2}{2}$, except at the value of u equal to the two coinciding singularities which is the superconformal point. In Section 5, we discuss the physics of this superconformal point in some detail. There, quite remarkably, one has *four* massless states, namely the quark $(n_e, n_m)_s = (1, 0)_1$ and the monopole $(0, 1)_0$ which are flavour doublets, and the two dyons $(1, 1)_1$ and $(-1, 1)_{-1}$ which are flavour singlets. This spectrum has an S-duality invariance which is realized by the monodromy matrix $M_{\rm sc}$ around the superconformal point. Since this massless sector constitutes the superconformal field theory, the latter should have a quantum S-duality invariance. We then discuss in general the Argyres-Douglas ansatz [6] for the β-function of a theory based on the massless states at the superconformal point. These authors conjecture that, although there is no local action at our disposal to simultaneously describe all massless states, the beta might nevertheless be obtained by simply computing the contribution of each massless particle in the formulation of the theory which describes it locally and then adding together the suitably duality transformed contributions. We show that despite its appealing features, this ansatz is not correct, as already suspected by these authors because it let to irrational values for the slope ω of the β-function at the fixed point. We argue that the slopes ω can be computed from the low-energy effective actions alone and find that they are a rational numbers related to the scaling dimensions α of $\langle \mathrm{tr}\, \phi^2 \rangle$ as $\omega = 2(\alpha - 1)$. We show that this relation is in perfect agreement with $N = 2$

superconformal invariance.

Then follow four appendices. In appendix A, we discuss the positions of the singularities and their different RG flows for $N_f = 1, 2$ and 3. In appendix B, we give details on the elliptic integrals needed in Section 2 - and heavily used for the numerical computations of Section 4. In appendix C, we express the period integrals in terms of the three elliptic integrals also for $N_f = 1, 3$ and for $N_f = 2$ with $m_1 = m,\ m_2 = 0$, and check the RG flows on these expressions. Finally, in appendix D, we study the RG flow of the $N_f = 2$ integrals with equal bare masses, thus providing some additional consistency checks.

2. RG flows, analytic structure, superconformal points and period integrals

The structure of the Coulomb branch of the asymptotically free SU(2) theories under study was derived in [1, 2]. It is given in terms of an elliptic curve of the form

$$y^2 = x^2(x-u) + P_{N_f}(x, u, m_j, \Lambda_{N_f}) \tag{2.1}$$

where[⋆] $u = \langle \mathrm{tr}\, \phi^2 \rangle$ is the gauge invariant moduli, ϕ the scalar component of the $N = 2$ vector multiplet, m_j $(1 \le j \le N_f)$ the bare masses of the hypermultiplets and Λ_{N_f} the dynamically generated scale of the theory. The polynomials P_{N_f} are given by

$$\begin{aligned}
P_0 =& \frac{\Lambda_0^4}{4}\, x\ , \\
P_1 =& \frac{\Lambda_1^3}{4}\, m_1 x - \frac{\Lambda_1^6}{64}\ , \\
P_2 =& -\frac{\Lambda_2^4}{64}\big(x-u\big) + \frac{\Lambda_2^2}{4} m_1 m_2 x - \frac{\Lambda_2^4}{64}(m_1^2 + m_2^2)\ , \\
P_3 =& -\frac{\Lambda_3^2}{64}\left(x-u\right)^2 - \frac{\Lambda_3^2}{64}\left(x-u\right)\big(m_1^2 + m_2^2 + m_3^2\big) \\
&+ \frac{\Lambda_3}{4} m_1 m_2 m_3 x - \frac{\Lambda_3^2}{64}\big(m_1^2 m_2^2 + m_1^2 m_3^2 + m_2^2 m_3^2\big)\ .
\end{aligned} \tag{2.2}$$

The masses of the so called BPS states, which come in short representations of the supersymmetry algebra, can be computed using the fundamental formula

$$M_{\mathrm{BPS}}(u) = \sqrt{2}\left| n_m a_D(u) - n_e a(u) + \sum_i s_i \frac{m_i}{\sqrt{2}} \right|. \tag{2.3}$$

In this expression, n_e and n_m are two integers representing the electric and magnetic charges of the state, and the s_i are integers or half-integers which correspond to constant parts of the

⋆ This relation is only valid up to a constant shift in the general case [13].

physical baryonic charges [2,8]. If λ is a meromorphic differential on the curve (2.1) such that

$$\frac{\partial\lambda}{\partial u} = \frac{\sqrt{2}}{8\pi}\,\frac{dx}{y} \tag{2.4}$$

then the variables a and a_D are given by the contour integrals

$$a = \oint_{\gamma_1} \lambda \quad , \quad a_D = \oint_{\gamma_2} \lambda \tag{2.5}$$

for a certain homology basis (γ_1, γ_2). The BPS mass formula (2.3) is compatible with duality transformations of the form

$$\begin{pmatrix} a_D \\ a \\ m/\sqrt{2} \end{pmatrix} \longrightarrow M \begin{pmatrix} a_D \\ a \\ m/\sqrt{2} \end{pmatrix} \quad , \quad \begin{pmatrix} n_e \\ n_m \\ s \end{pmatrix} \longrightarrow M^* \begin{pmatrix} n_e \\ n_m \\ s \end{pmatrix} \tag{2.6}$$

where

$$M = \begin{pmatrix} \alpha & \beta & f \\ \gamma & \delta & g \\ 0 & 0 & 1 \end{pmatrix} \quad , \quad M^* = \begin{pmatrix} \alpha & \beta & 0 \\ \gamma & \delta & 0 \\ \alpha g - \gamma f & \beta g - \delta f & 1 \end{pmatrix} \tag{2.7}$$

with α, β, γ, δ integers such that $\det M = 1$ and f, g integers or half-integers. Note the useful relations

$$\big(M_1 M_2\big)^* = M_1^* M_2^* \quad , \quad \big(M^*\big)^{-1} = \big(M^{-1}\big)^* \, . \tag{2.8}$$

One particularly important class of duality transformations corresponds to the monodromy transformations a and a_D undergo when encircling a singularity in the u plane. These singularities are due to dyons $(n_e, n_m)_s^{\times d}$ lying in a d-dimensional representation of the flavour group becoming massless and occur when the curve (2.1) has a vanishing cycle, i.e. when the discriminant of the corresponding polynomial (2.2) vanishes. When all the *non-zero* bare masses are equal, which is the only case we will study in the following for the seek of simplicity, the mass term in (2.3) is of the form $ms/\sqrt{2}$, and the monodromy matrices then read

$$\begin{aligned} M_{(n_e,n_m)_s^{\times d}} &= \begin{pmatrix} 1 - dn_e n_m & dn_e^2 & -dn_e s \\ -dn_m^2 & 1 + dn_m n_e & -dn_m s \\ 0 & 0 & 1 \end{pmatrix} \, , \\ M^*_{(n_e,n_m)_s^{\times d}} &= \begin{pmatrix} 1 - dn_e n_m & dn_e^2 & 0 \\ -dn_m^2 & 1 + dn_m n_e & 0 \\ -dsn_m & dsn_e & 1 \end{pmatrix} \, . \end{aligned} \tag{2.9}$$

When two singularities coincide, the monodromy is given by the product of two matrices of the type (2.9). Note that the fact that a and a_D pick up constants multiple of $m/2\sqrt{2}$ under

monodromy transformations is possible because the differential λ has poles with residues such that

$$2\pi i \ \mathrm{res}\lambda = \sum_i t_i \frac{m_i}{\sqrt{2}} \ , \quad t_i \in \frac{1}{2}\mathbf{Z} \ . \tag{2.10}$$

2.1. **RG flows and superconformal points**

The theories for different N_f are related by the renormalization group flow when some of the bare masses of the hypermultiplets are sent to infinity and the corresponding states can be integrated out (see Appendices A and C). For instance, if we let $m_3 \to \infty$ while keeping $\Lambda_2^2 = m_3\Lambda_3$ fixed, the polynomial P_3 in (2.2) flows to P_2. Another flow which we will study in great details in the following is $m_1 = m_2 = m \to \infty$ with $m\Lambda_2 = \Lambda_0^2$ fixed which allows to obtain the $N_f = 0$ theory directly from the $N_f = 2$ theory. A particularly important phenomenon that must occur during the RG flow is that the quantum numbers of some of the particles becoming massless change. Typically, when $m \to \infty$ some singularities are at weak coupling and correspond to elementary quarks becoming massless while when $m \to 0$ these singularities move towards the strongly coupled region where only magnetically charged states can become massless. The transformation of the quantum numbers must be implemented by a $\mathrm{SL}(2,\mathbf{Z})$ matrix U. Since the electric and magnetic quantum numbers of the singularities at $m = 0$ can in general be deduced on physical grounds, by using for instance the discrete symmetry acting on the Coulomb branch when it exists, the general form of U can be determined a priori. Two cases can then arise: either the matrix U does or does not correspond to any monodromy matrix of the form (2.9). If it does not, we will see that (for real m) the quantum numbers change when at least two singularities coincide. Such points were discovered by inspection in [7]. The low energy theory at these points is believed to correspond to an interacting $N = 2$ superconformal theory [6,7]. We will discuss the physics of these theories in Section 5, but let us right now display the monodromy matrix around such a superconformal point, discuss some general constraints that it must satisfy in order to be compatible with conformal invariance, and determine the way the quantum numbers of the singularities change.

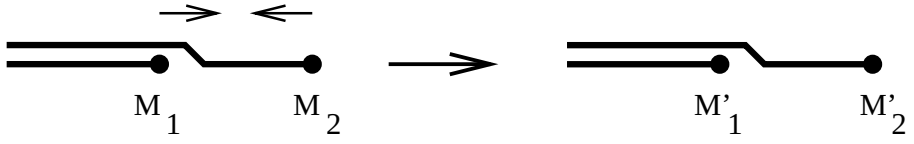

Fig. 1: After the collision, the quantum numbers at the singularities and thus the associated monodromy matrices change according to equations (2.15) or (2.16).

The generic case of two colliding singularities σ_1 and σ_2 is represented in Fig. 1. The singularity σ_j whose monodromy is M_j is due to d_j hypermultiplets $(p_j, q_j)_{s_j}$ becoming massless. Note that we choose σ_1 to be below the cut produced by σ_2. If the two cuts actually coincide on the left of σ_1, this will mean that the quantum numbers $(p_1, q_1)_{s_1}$ at σ_1 are computed by

looking at the solution (a_D, a) below the cut. With this convention, the monodromy at the superconformal point is

$$M_{\rm sc} = M_2 M_1. \tag{2.11}$$

The eigenvalues of this matrix depend on one symplectic invariant integer parameter

$$k = d_1 d_2 (p_1 q_2 - p_2 q_1)^2 \tag{2.12}$$

which is such that $\mathrm{tr}\, M_{\rm sc} = 2 - k$. We must have $k > 0$ since otherwise the particles becoming massless are mutually local and the low energy theory is simply $N = 2$ super QED with a dual photon. Superconformal invariance implies that the dimensions of a and a_D must both be equal to one, and thus that near the superconformal point u_* the following expansion is valid

$$\begin{aligned} a_D(u) =& a_D(u_*) + c_D (u - u_*)^{1/\alpha} + o\big((u-u_*)^{1/\alpha}\big) \\ a(u) =& a(u_*) + c (u - u_*)^{1/\alpha} + o\big((u-u_*)^{1/\alpha}\big), \end{aligned} \tag{2.13}$$

where c_D and c are constants and α is the anomalous dimension of the operator u. This is possible only if the eigenvalues of $M_{\rm sc}$ are of modulus one, which rules out the cases $k > 4$. Moreover, when $k = 4$, $M_{\rm sc}$ is, up to a global sign, conjugate to a certain non-zero power of T. This would be the signal of logarithmic terms in the asymptotic expansion of a and a_D, which again are ruled out by conformal invariance. Thus we conclude that $1 \leq k \leq 3$. The three allowed values of k correspond to three inequivalent SCFT. We will bring some evidence in Section 4 that the SCFT is actually (fully) characterized by this integer k, by computing critical exponents as functions of k.

Denoting with a prime the quantities corresponding to the new quantum numbers after the collision of the singularities, as indicated in Fig. 1, one must have

$$M_2 M_1 = M_2' M_1'. \tag{2.14}$$

The multiplicity d_j of a given singularity σ_j, which can be directly read off the discriminant of the relevant polynomial (2.1), (2.2), cannot change at the superconformal point. Thus one must either have $d_j = d_j'$, in which case (2.14) can be solved non trivially by

$$M_j' = U M_j U^{-1}, \quad \text{with} \quad U = M_{sc}^{-1}, \tag{2.15}$$

or $d_1' = d_2$, $d_2' = d_1$, in which case (2.14) can be solved by

$$M_1' = U M_2 U^{-1}, \quad M_2' = U M_1 U^{-1}, \quad \text{with} \quad U = M_1^{-1} \quad \text{or} \quad U = M_2. \tag{2.16}$$

The quantum numbers are then changed according to the matrix U^*, see (2.7). When $k = 3$, there is another consistent solution to (2.14), which corresponds to $U = I + M_{\rm sc}^{-1}$ if $d_j = d_j'$ or to $U = M_1^{-1} + M_2$ if $d_1' = d_2$. The matrix U is then not of the form (2.7), but its 2×2 upper

left block part is still in $\mathrm{SL}(2,\mathbf{Z})$.[⋆] The corresponding matrix U^* can then be straightforwardly deduced by equating the central charges of the original and image states. This latter case, with $d_1' = d_2$, is actually realized in the $N_f = 3$ theory with three equal masses which we study in the next subsection.

2.2. **RG flows and analytic structure**

In Fig. 2, we have reprensented three different RG flows which illustrate the discussion of the previous subsection.

The first case corresponds to the flow from the $N_f = 2$ theory to the $N_f = 1$ theory obtained by sending m_2 to infinity while keeping $m_2\Lambda_2^2 = \Lambda_3^3$ fixed, and $m_1 = 0$. No superconformal point is needed in this case. The dyon singularity $(1,1)_1$ changes to one component of the elementary quark $(1,0)_1$ when crossing the cut produced by the $(0,1)_0$ singularity as m_2 is increased. In order to recover a more conventional analytic structure in the $m_2 \to \infty$ limit, one can move the cut originating at $(1,0)_1$ to the right as indicated in the Figure. Physically, this simply amounts to shifting the θ angle by an integer multiple of 2π in the upper half u-plane, which is an unphysical transformation. Mathematically, one keeps the solution (a_D, a) fixed for $\Im m\, u < 0$ and performs the transformation

$$\begin{pmatrix} a_D \\ a \\ m/\sqrt{2} \end{pmatrix} \longrightarrow M^{-1}_{(1,0)_1} \begin{pmatrix} a_D \\ a \\ m/\sqrt{2} \end{pmatrix} \tag{2.17}$$

for $\Im m\, u > 0$. It follows that the quantum numbers of the massless state at the singularity which were $(0,1)_1$ before, now are $\left(M^{-1}_{(1,0)_1}\right)^* (0,1)_1 = (-1,1)_0$.

The second case corresponds to the flow from the $N_f = 3$ theory with three equal bare masses $m_1 = m_2 = m_3 = m$ to the pure gauge theory $N_f = 0$. Let us discuss in this case the quantum numbers of the singularities in more detail. When $m = 0$, one has two singularities. One of them is due to a dyon $(1,1)$ lying in the spinorial representation **4** of the flavour group Spin(6)=SU(4). A basis for this representation can be taken to be $(|0\rangle, \psi_i^\dagger \psi_j^\dagger |0\rangle)$ where the $\psi_i^\dagger$, $1 \le i \le N_f = 3$, are the fermionic zero modes carrying flavour indices and one unit of s_i charge.[†] With this convention, all states with $n_m = 1$ and odd electric charge will lie in the same spinorial representation **4**, while states with $n_m = 1$ and even n_e will lie in the other, complex conjugate, spinorial representation $\mathbf{4}^*$. The second singularity is due to a $n_m = 2$ flavour singlet dyon. When $n_m = 2$, the number of fermionic zero modes is doubled and one

⋆ This would not be the case for $k = 1$ or $k = 2$.

† A semiclassical analysis is valid for studying the flavour symmetry properties of the states becoming massless even at strong coupling because these states can be continuously transported to weak coupling by varying u.

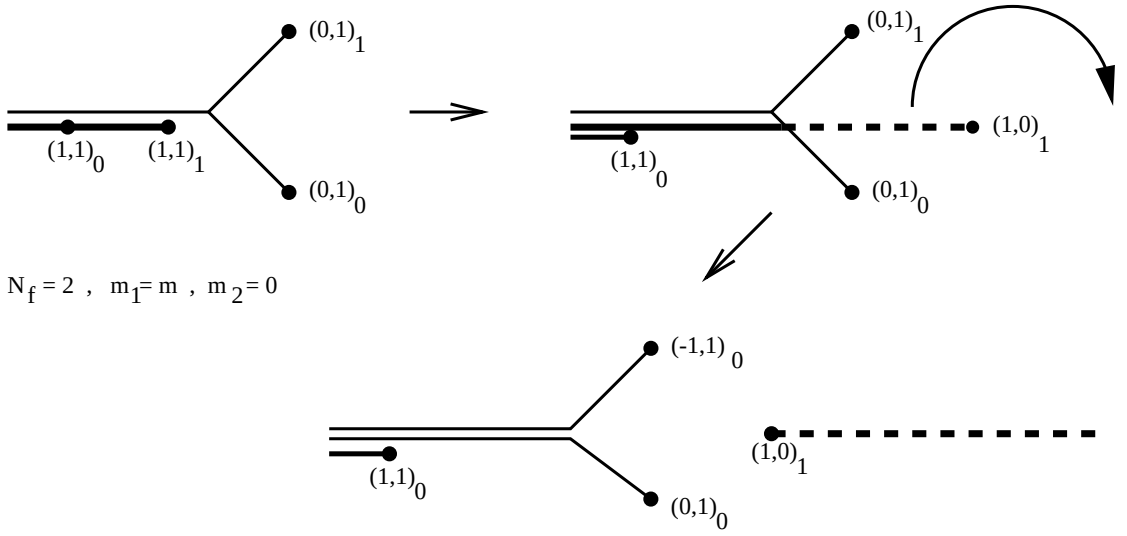

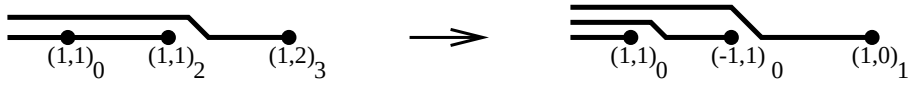

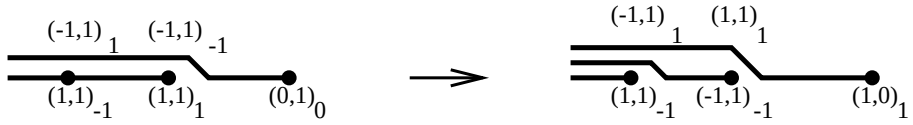

Fig. 2: Shown are three different RG flows from N_f to $N_f' < N_f$, $m \to \infty$, $\Lambda_{N_f} \to 0$ with $\Lambda_{N_f'}^{4-N_f'} = \Lambda_{N_f}^{4-N_f} m^{N_f - N_f'}$ fixed. The upper figure gives the flow from $N_f = 2$ to $N_f' = 1$, the middle figure the flow $N_f = 3$ to $N_f' = 0$ and the lower one $N_f = 2$ to $N_f' = 0$. In this latter case which will be studied in detail in Section 4, we have indicated the quantum numbers of the singularities on *both* sides of the branch cuts.

can indeed construct SU(4) singlets from the $\mathbf{4} \otimes \mathbf{4}^*$ tensor product. The ket associated with $(1, 2)$ is then of the form

$$|\psi\rangle = \left(\psi_1^{a\dagger}\psi_2^{a\dagger}\psi_3^{a\dagger} + \psi_1^{a\dagger}\psi_2^{b\dagger}\psi_3^{b\dagger} + \psi_1^{b\dagger}\psi_2^{a\dagger}\psi_3^{b\dagger} + \psi_1^{b\dagger}\psi_2^{b\dagger}\psi_3^{a\dagger}\right)|0\rangle \tag{2.18}$$

with $1 \leq a, b \leq 2$ and $a \neq b$. Let s_0 be the $s = \sum s_i$ charge of $|0\rangle$. When $m > 0$, the flavour symmetry group is broken from SU(4) to SU(3). We see that the $(1,1)$ singularity will then split into one SU(3) singlet of s charge s_0, $(1,1)_{s_0}$, and one SU(3) vector of s charge $s_0 + 2$, $(1,1)_{s_0+2}$. As for the $(1,2)$ singularity, is must be a SU(3) singlet of s charge $s_0 + 3$. At the expense of shifting the variables a_D and a by integer multiples of $m/\sqrt{2}$, that is to say choosing the cycles (γ_1, γ_2) in (2.5) so that they encircle the poles with non zero residues of the Seiberg-Witten differential λ an appropriate number of times, we can always choose $s_0 = 0$ as in Fig. 2, and the singularities are $(1,1)_0$, $(1,1)_2$ and $(1,2)_3$. This is a natural choice because for example the $(1,1)_0$ state must remain stable and of finite mass for any u when $m \to \infty$. This choice of s charges will then insure that the solution (a_D, a) for the $N_f = 3$ theory will flow smoothly towards the solution for the pure gauge theory, without picking any (infinite) shift proportional to m. When $m = \Lambda_3/8$, we reach a $k = 3$ superconformal point where the triplet $(1,1)_2^{\times 3}$ and the singlet $(1,2)_3$ cross. Using the formula (2.16) with $U = M^{-1}_{(1,1)_2^{\times 3}} + M_{(1,2)_3}$, we see that the singlet $(1,2)_3$ becomes the dyon $(-1,1)_0$ and the triplet $(1,1)_2$ becomes the quark $(1,0)_1$. This is exactly what one would expect on physical grounds. Note that we could have deduced that the s charge of $(1,2)$ must be 3 independently of the previous semiclassical reasoning by requiring that the elementary quark must have $s = 1$.

Finally, the third case we have depicted in Fig. 2 is the flow of the $N_f = 2$ theory with equal bare masses towards the pure gauge theory. This case will be extensively studied in Section 4. In particular, we will determine the existence domains of all the BPS states along this flow. In the figure, we have also indicated the quantum numbers of the singularities as viewed from the upper half u-plane. We have a $k = 2$ superconformal point when $m = \Lambda_2/2$. In the present case, the singlet and doublet collide but do not cross each other and we are in the situation of eq. (2.15) with $U = M_{\rm sc}^{-1} = \left(M_{(0,1)_0} M_{(1,1)_1}\right)^{-1}$. Note that the upper left block of U, acting on (n_e, n_m) is nothing but the matrix $-S = \begin{pmatrix} 0 & -1 \\ 1 & 0 \end{pmatrix}$. Note also that our choice of s charges is not in this case the most natural from the point of view of the RG flow. We prefered to make easier the implementation of CP invariance which we will use when determining the BPS spectra, by choosing a solution (a_D, a) satisfying

$$a_D(\overline{u}) = -\overline{a}_D(u), \quad a(\overline{u}) = \overline{a}(u). \tag{2.19}$$

Then the transformation law of the quantum numbers under CP is simply

$$(n_e, n_m)_s \xrightarrow{\rm CP} (-n_e, n_m)_{-s}. \tag{2.20}$$

2.3. **The computation of the period integrals**

In the following, we will need explicit expressions for the periods a_D and a, in order to compute the curves of marginal stability which determine the existence domains of the stable BPS states. A general method, first introduced and used in [8], and also independently in [12], simply consists in expanding the period integrals a_D and a in terms of the three fundamental elliptic integrals, which can be expressed in terms of standard special functions well suited for a numerical computation. An efficient way of taking care of the precise definition of the cycles (γ_1, γ_2) is to uniformize the cubics (2.1) with the help of the Weirstraß $\wp$ function. For a cubic curve in Weierstraß normal form, i.e.

$$\eta^2 = 4\prod_{i=1}^{3}(\xi - e_i) \ , \quad \sum_{i=1}^{3} e_i = 0 \tag{2.21}$$

the three fundamental elliptic integrals are

$$I_1^{(j)} = \oint\limits_{\gamma_j} \frac{\mathrm{d}\xi}{\eta} \ , \quad I_2^{(j)} = \oint\limits_{\gamma_j} \frac{\xi \mathrm{d}\xi}{\eta} \ , \quad I_3^{(j)}(c) = \oint\limits_{\gamma_j} \frac{\mathrm{d}\xi}{\eta(\xi - c)} \cdot \tag{2.22}$$

By convention, we choose the cycle γ_1 to encircle e_3 and e_2, and the cycle γ_2 to encircle e_1 and e_2. Of course, we still need to specify how we choose to number the three roots e_i in each particular case. Sometimes, if we do not specify the contours, we simply write I_1 for $\int \frac{\mathrm{d}\xi}{\eta}$ etc.

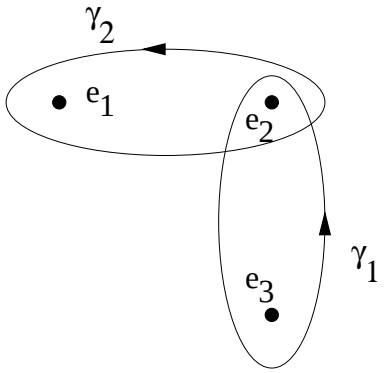

Fig. 3: The definition of the basic cycles γ_1 and γ_2 with respect to the roots e_1, e_2 and e_3.

The necessity to introduce the elliptic integral of the third kind I_3 is due to the presence of poles with non-zero residues in the massive theories. This also explains the failure of the standard methods of computation of the periods by means of the Picard-Fuchs equations. For the massless theories only I_1 and I_2 occur which can be reexpressed in terms of hypergeometric functions.

Let us focus on the case $N_f = 2$ with $m_1 = m_2 = m$. The other cases are discussed in Appendix C. The Seiberg-Witten differential $\lambda \equiv \lambda^{N_f=2}_{m_1=m_2=m}$ is given by

$$\begin{aligned}\lambda &= -\frac{\sqrt{2}}{4\pi}\frac{y\,\mathrm{d}x}{x^2-\frac{\Lambda_2^4}{64}} = -\frac{\sqrt{2}}{4\pi}\frac{\mathrm{d}x}{y}\frac{4y^2}{\Lambda_2^2}\left(\frac{1}{x-\frac{\Lambda_2^2}{8}}-\frac{1}{x+\frac{\Lambda_2^2}{8}}\right)\\ &= -\frac{\sqrt{2}}{4\pi}\frac{\mathrm{d}x}{y}\left[x-u+\frac{\Lambda_2^2}{4}\frac{m^2}{x+\frac{\Lambda_2^2}{8}}\right]\,.\end{aligned} \tag{2.23}$$

Converting to Weierstraß normal form of the cubic by $\eta = 2y,\ \xi = x - \frac{u}{3}$ we arrive at

$$\oint_{\gamma_i}\lambda = \frac{\sqrt{2}}{4\pi}\left[\frac{4}{3}u\,I_1^{(i)} - 2\,I_2^{(i)} - \frac{\Lambda_2^2}{2}m^2\,I_3^{(i)}\left(-\frac{\Lambda_2^2}{8}-\frac{u}{3}\right)\right]\,. \tag{2.24}$$

One sees from (2.23) that λ has two poles at $(x = \frac{-\Lambda_2^2}{8}, y = \pm\frac{i}{4}m\Lambda_2^2)$ with residues $\mp\frac{1}{2\pi i}\frac{m}{2\sqrt{2}}$ [2].

In order to have an explicit formula for a_D and a, we now have to choose the roots e_j of the polynomial defining the cubic. One constraint comes from the asymptotic behaviour for large $|u|$, which is governed by asymptotic freedom:

$$a(u) \sim \frac{1}{2}\sqrt{2u}\,, \quad a_D(u) \sim \frac{i}{2\pi}\sqrt{2u}\log\frac{u}{\Lambda_2^2}. \tag{2.25}$$

Since $a(u)$ is given by the integral over the cycle γ_1 surrounding e_2 and e_3, see Fig 3, the *set* $\{e_2, e_3\}$ must be chosen such that the large-u asymptotics of a does *not* contain a $\sqrt{2u}\log u/\Lambda^2$ term. The remaining root necessarily is e_1. But which root in the set $\{e_2, e_3\}$ is called e_2, and thus is encircled also by γ_2, is a matter of convention related to the possibility of shifting a_D by an integer multiple of a. A correct choice is the following

$$\begin{aligned}e_1 &= \frac{u}{6} - \frac{\Lambda_2^2}{16} + \frac{1}{2}\sqrt{u+\frac{\Lambda_2^2}{8}+\Lambda_2 m}\sqrt{u+\frac{\Lambda_2^2}{8}-\Lambda_2 m}\,,\\ e_2 &= -\frac{u}{3} + \frac{\Lambda_2^2}{8}\,,\\ e_3 &= \frac{u}{6} - \frac{\Lambda_2^2}{16} - \frac{1}{2}\sqrt{u+\frac{\Lambda_2^2}{8}+\Lambda_2 m}\sqrt{u+\frac{\Lambda_2^2}{8}-\Lambda_2 m}\,.\end{aligned} \tag{2.26}$$

One can then straightforwardly show (see Appendix D) that in the limit $m \to 0$ the solution given by (2.5) and (2.24) converges toward the already known explicit solution of the massless $N_f = 2$ theory [4] which also corresponds to the electric and magnetic quantum numbers at the singularities chosen in Fig. 2. It still remains to fix the positions of the cycles relatively

to the poles with nonzero residues of λ, or, which is equivalent, to fix the s charges at the singularities. The solution, consistent with Fig. 2, is given for $\Im m\, u > 0$ by

$$\begin{aligned} a(u) &= \frac{\sqrt{2}}{4\pi}\left[\frac{4}{3}\,uI_1^{(1)} - 2\,I_2^{(1)} - \frac{\Lambda_2^2}{2}m^2\,I_3^{(1)}\left(-\frac{\Lambda_2^2}{8} - \frac{u}{3}\right)\right] + \frac{m}{\sqrt{2}} \\ a_D(u) &= \frac{\sqrt{2}}{4\pi}\left[\frac{4}{3}\,uI_1^{(2)} - 2\,I_2^{(2)} - \frac{\Lambda_2^2}{2}m^2\,I_3^{(2)}\left(-\frac{\Lambda_2^2}{8} - \frac{u}{3}\right)\right] \end{aligned} \tag{2.27}$$

with the $I_j^{(1)}$ precisely given by the formulae

$$\begin{aligned} I_1^{(1)} =& \frac{2}{(e_1-e_3)^{1/2}}\,K(k) \\ I_2^{(1)} =& \frac{2}{(e_1-e_3)^{1/2}}\,\left[e_1K(k) + (e_3-e_1)E(k)\right] \\ I_3^{(1)} =& \frac{2}{(e_1-e_3)^{3/2}}\left[\frac{1}{1-\tilde{c}+k'}\,K(k)\right. \\ & \left. + \frac{4k'}{1+k'}\,\frac{1}{(1-\tilde{c})^2-k'^2}\,\Pi_1\left(\nu(c), \frac{1-k'}{1+k'}\right)\right] \end{aligned} \tag{2.28}$$

where

$$\begin{aligned} k^2 = \frac{e_2-e_3}{e_1-e_3}\;, \quad k'^2 = 1-k^2 = \frac{e_2-e_1}{e_3-e_1}\;, \\ \tilde{c} = \frac{c-e_3}{e_1-e_3}\;, \quad \nu(c) = -\left(\frac{1-\tilde{c}+k'}{1-\tilde{c}-k'}\right)^2\left(\frac{1-k'}{1+k'}\right)^2\;, \end{aligned} \tag{2.29}$$

and the $I_j^{(2)}$ obtained form the $I_j^{(1)}$ by exchanging e_1 and e_3. In (2.28), K, E and Π_1 are the three standard elliptic integrals of [14] whose integral representations are given in Appendix B. For $\Im m\, u < 0$ the solution then is obtained from (2.19). In Appendix B we derive eqs. (2.28) as well as some useful relations between the elliptic integrals. In Appendix D, we discuss in some detail how one can understand the RG flow illustrated in Fig. 2 directly from the explicit formulae (2.27). In particular, as $m \to \infty$, $m\Lambda_2 = \Lambda_0^2$ fixed, we have

$$a(u) \to a^{(0)}(u) \quad , \quad \tilde{a}_D(u) \to a_D^{(0)}(u) \quad , \quad \text{where} \quad \tilde{a}_D(u) = a_D(u) - \epsilon a(u) + \epsilon\frac{m}{\sqrt{2}}\;. \tag{2.30}$$

Here and in the following we always let $\epsilon = \mathrm{sign}(\Im m\, u)$. The redefinition $a_D \to \tilde{a}_D$ corresponds to rotating the cut originating from the massless quark singularity σ_3 to the right (and changing the contour γ_2). This is what one wants since this cut must disappear in the $m \to \infty$ limit in order to recover the standard analytic structure of the pure gauge theory.

3. The spectra of stable BPS states

3.1. Decay curves

In general, a given BPS state does not exist everywhere on the Coulomb branch of the moduli space. For each of the *massless* theories with $N_f \leq 3$ [4,3] there is a single curve of marginal stability which goes through the singularities and separates the Coulomb branch into two regions. In the region outside this curve all semiclassically stable states exist, while inside the curve only those BPS states exist that are responsible for the singularities, in addition to the photon vector multiplet.

The present cases of hypermultiplets with non-vanishing bare masses are very different. Due to the BPS mass formula $M_{\rm BPS} = \sqrt{2}|Z|$ with

$$Z(u) = n_m a_D(u) - n_e a(u) + \sum_{i=1}^{N_f} s_i \frac{m_i}{\sqrt{2}} \tag{3.1}$$

a BPS state is stable against any decay of the type

$$(n_e, n_m)_{s_i} \to k \times (n'_e, n'_m)_{s'_i} + l \times (n''_e, n''_m)_{s''_i} \tag{3.2}$$

($k, l \in \mathbf{Z}$) unless this satisfies at the same time the conservation of charges and of the total BPS mass:

$$n_e = kn'_e + ln''_e \quad , \quad n_m = kn'_m + ln''_m \quad , \quad s_i = ks'_i + ls''_i \quad \Rightarrow \quad Z = k\,Z' + l\,Z'' \tag{3.3}$$

and

$$|Z| = |k\,Z'| + |l\,Z''| \tag{3.4}$$

with obvious notations for Z' and Z''. If all bare masses m_i are equal, due to the $\mathrm{SU}(N_f)$ flavour symmetry, only the sum $s = \sum_i s_i$ is relevant and needs to be conserved. We see that a decay that satisfies the charge conservations (3.3) is possible only if

$$\frac{Z'}{Z} \equiv \zeta \in \mathbf{R} \ , \tag{3.5}$$

and moreover if it is kinematically possible, i.e. if

$$0 \leq k\zeta \leq 1 \ . \tag{3.6}$$

For the case of vanishing bare masses, $m_i = 0$ condition (3.5) reduces to $\Im m\, \frac{a_D(u)}{a(u)} = 0$ which yields a single curve $\mathcal{C}^0$ on the Coulomb branch independent of the initial state $(n_e, n_m)_{s_i}$ considered. For non-vanishing bare masses however, we have a whole family of possible decay

curves. Moreover, a priori, there is a different family of such curves for each BPS state. As an example consider a dyon with $n_m = 1$. Then condition (3.5) reads

$$\Im m \ \frac{n'_m a_D - n'_e a + \sum_i s'_i \frac{m_i}{\sqrt{2}}}{a_D - n_e a + \sum_i s_i \frac{m_i}{\sqrt{2}}} = 0 \ \Leftrightarrow \ \Im m \ \frac{-(n'_e - n'_m n_e)a + \sum_i (s'_i - n'_m s_i)\frac{m_i}{\sqrt{2}}}{a_D - n_e a + \sum_i s_i \frac{m_i}{\sqrt{2}}} = 0 \ . \quad (3.7)$$

For fixed n_e and s_i, this is an N_f-parameter family of curves with rational parameters $r_i = (n'_e - n'_m n_e)/(s'_i - n'_m s_i)$. Even though there are some relations between the possible quantum numbers n'_e and s'_i, n'_m (see next subsection) there are still many possible values of r_i and we expect a multitude of curves of marginal stability on the Coulomb branch of moduli space resulting in a rather chaotic situation. Fortunately not all of these curves satisfy the additional criterion (3.6). In particular, for the case we will study in detail in the next section, namely $N_f = 2$ with equal bare masses, where one expects a different one-parameter family of curves labelled by $r = (n'_e - n'_m n_e)/(s' - n'_m s)$, $s = s_1 + s_2$, for *each* BPS state, it turned out that only one or two such curves in each family are relevant, i.e. satisfy the additional criterion (3.6). Hence the set of all relevant curves for *all* BPS states are nicely described by a single set of curves $\mathcal{C}^{\pm}_{2n}$, $n \in \mathbf{Z}$, and rather than having a chaotic situation one gets a very clear picture of which states exist in which region of the Coulomb branch. It will become clear that this organizing scheme should be similarly at work for all other massive theories with $N_f \leq 3$.

One particularly simple case is the decay of states with $\sum s_i m_i = 0$ into states with $\sum s'_i m_i = 0$. The corresponding decay curves all are given by $\Im m \, \frac{a_D(u)}{a(u)} = 0$, i.e. they all coincide with the curve $\mathcal{C}^0$. We will see that this is quite an important case, and that this curve $\mathcal{C}^0$ still plays a priviledged rôle, even for non-zero bare masses.*

Note that if we had considered decays into three independent BPS states, $(n_e, n_m)_{s_i} \to k \times (n'_e, n'_m)_{s'_i} + l \times (n''_e, n''_m)_{s''_i} + q \times (n'''_e, n'''_m)_{s'''_i}$, we would have *two* conditions: eq. (3.5) would be supplemented by $\frac{Z''}{Z} \in \mathbf{R}$, so that such "triple" decays can only occur at the intersection *points* of two curves. Below, when we discuss how to transport a BPS state along a path from one region to another, the path can always be chosen so as to avoid such intersection points. Hence, triple decays are irrelevant for establishing the existence domains of the BPS states. Obviously, "quadruple" and higher decays, if possible at all, are just as irrelevant.

$\star$ This statement is of course meant for the choice of a_D and a that gives finite limits under the RG flow as $m \to \infty$. For $N_f = 2$ with equal masses, these are the $\tilde{a}_D$ and a of eq. (2.30) and $\sum s_i m_i = \sum s'_i m_i = 0$ is meant to be $\tilde{s} = \tilde{s}' = 0$.

3.2. **Our working hypothesis**

In order to determine the BPS spectra at any point on the Coulomb branch, we will extensively use the following claim:

P: *At any point of the Coulomb branch of a theory having N_f flavours with bare masses m_j, $1 \leq j \leq N_f$, the set of stable BPS states is included into the set of stable BPS states of the $m_j = 0$ theory at weak coupling.*

Note that the Coulomb branch of the $m_j = 0$ theory is separated into two regions, one containing all the BPS states stable at weak coupling, and the other at strong coupling containing a finite subset of the BPS states stable at weak coupling [3,4]. One simple consequence of the claim (P) is that the set of stable BPS states cannot enlarge when one goes from the N_f to the $N_f - 1$ theory following the RG flow which is what one naturally expects. This is perfectly consistent with the spectra determined for zero bare masses in [3,4]. Another consequence, which plays a prominent rôle in the present work, is that the possible decay reactions between BPS states are then extremely constrained and thus the number of relevant curves of marginal stability enormously decreased. This is explained in detail for the $N_f = 2$ theory with two equal bare masses $m_1 = m_2 = m$ in the next section.

Let us give a strong argument motivating our fundamental claim (P). It is inspired of ideas already discussed in [11]. A crucial fact is that, for any BPS state $p = (n_e, n_m)_s$ which does not belong to the weak coupling spectrum of the $m_j = 0$ theory, there always exist some values of the m_j for which

$$n_m a_D(u_0, m_j) - n_e a(u_0, m_j) + s\frac{m}{\sqrt{2}} = 0 \tag{3.8}$$

at some non-singular u_0 on the Coulomb branch. This may be proven by noting that for sufficiently large $|m_j|$, the point u_0, if it exists, lies at large $|u| \sim |m_j|$ where the formulas for a_D and a simplify and thus where (3.8) can be studied very explicitly. The set of curves of marginal stability $\cup_{r\in\mathbf{Q}}\mathcal{C}_p(r, m_j)$ a priori relevant for the decays of $p = (n_e, n_m)_s$, all cross at the point u_0 and form a dense subset of the Coulomb branch. The same properties are true for the complementary set $\cup_{r\in(\mathbf{R}\setminus\mathbf{Q})}\mathcal{C}_p(r, m_j)$. Now, suppose that p exists in some open set of the Coulomb branch. It must then exist at some points on a curve $\mathcal{C}_p(r, m_j)$ with r an irrational number. Since the state p cannot decay on such a curve for r irrational, it must also exist at the point u_0 where it is massless, which would contradict the fact that u_0 is not a singular point. Thus p cannot exist as a stable state in any open region for the values of m_j such that (3.8) has a solution. Now, by varying the m_j, the curves $\mathcal{C}_p(r, m_j)$ loose their shape and will no longer cross at a single point , but we are still insured that p cannot exist on any $\mathcal{C}_p(r, m_j)$ with r irrational. We believe on physical grounds that the fact that p cannot exist in any open region of the Coulomb branch means that p simply cannot exist at all as a stable BPS state. Finally, note that instead of studying eq. (3.8), we could remark that for arbitrarily small $|m_j|$, the spectra of BPS states should be the same as the one for the $m_j = 0$ theory, which proves that an undesirable state like p cannot exist on $\mathcal{C}_p(r, m_j)$ for r irrational and sufficiently

small $|m_j|$, and thus for any m_j. However, this reasoning certainly is less rigorous than the one based on (3.8). To end this section, let us point out that the claim (P) is also strongly supported by the stringy approach used in [10].

4. The case of two flavours with equal masses

As an illustrative and representative example, in this section we study the BPS spectra of the $N_f = 2$ theory with any $m_1 = m_2 = m$ real positive bare mass in great detail. The analytic structures for small ($0 < m < \Lambda_2/2$) and large ($m > \Lambda_2/2$) bare masses is displayed in the lower Fig. 2, while the explicit solution for the periods a_D and a is given by equations (2.27) . The three singularities on the Coulomb branch are at points $u = \sigma_j$, $\sigma_1 \leq \sigma_2 \leq \sigma_3$, such that

$$\sigma_1 = -\frac{\Lambda_2^2}{8} - \Lambda_2 m \ , \quad \sigma_2 = -\frac{\Lambda_2^2}{8} + \Lambda_2 m \ , \quad \sigma_3 = m^2 + \frac{\Lambda_2^2}{8}. \tag{4.1}$$

When $m = \Lambda_2/2$, the singularities σ_2 and σ_3 coincide. For small mass, $0 < m < \Lambda_2/2$, the monodromies M^* (see (2.9)) as viewed from the lower half u-plane are given by

$$M_1^* = \begin{pmatrix} 0 & 1 & 0 \\ -1 & 2 & 0 \\ 1 & -1 & 1 \end{pmatrix} \ , \quad M_2^* = \begin{pmatrix} 0 & 1 & 0 \\ -1 & 2 & 0 \\ -1 & 1 & 1 \end{pmatrix} \ , \quad M_3^* = \begin{pmatrix} 1 & 0 & 0 \\ -2 & 1 & 0 \\ 0 & 0 & 1 \end{pmatrix} \ , \tag{4.2}$$

while for $m > \Lambda_2/2$,

$$M_1^* = \begin{pmatrix} 0 & 1 & 0 \\ -1 & 2 & 0 \\ 1 & -1 & 1 \end{pmatrix} \ , \quad M_2^* = \begin{pmatrix} 2 & 1 & 0 \\ -1 & 0 & 0 \\ 1 & 1 & 1 \end{pmatrix} \ , \quad M_3^* = \begin{pmatrix} 1 & 2 & 0 \\ 0 & 1 & 0 \\ 0 & 2 & 1 \end{pmatrix} \ . \tag{4.3}$$

The monodromy at the superconformal point, according to (2.11), is given by

$$M_{\rm sc}^* = M_{2\cdot 3}^* = M_3^* M_2^* = \begin{pmatrix} 0 & 1 & 0 \\ -1 & 0 & 0 \\ -1 & 1 & 1 \end{pmatrix} \tag{4.4}$$

Before embarking on the detailed derivation of the BPS spectra, let us first discuss what one expects from the RG flow arguments. For $m = 0$ there is a single decay curve, and outside this curve all semiclassical states exist, namely all dyons $(n, 1)$ and the W-boson $(2, 0)$ as well as the quarks $(1, 0)$. The dyons are doublets in one or the other spinor representation of the flavour spin(4) group, while the quarks are in the vector representation and the W-boson is a singlet. Inside the curve, only the states that can become massless and are responsible for the singularities exist, namely the monopole $(0, 1)$ and the dyon $(-\epsilon, 1)$. As soon as a non-zero bare mass m is turned on, the s-charge becomes relevant, and certain multiplets split.

Semiclassically we still have doublets of dyons $(2n,1)_0$ with even n_e and $s=0$, while the doublets with odd n_e split into two singlets $(2n+1,1)_{+1}$ and $(2n+1,1)_{-1}$. We have a quark doublet $(1,0)_1$ and another quark doublet $(1,0)_{-1}$, as well as the W-boson $(2,0)_0$. According to our claim (P), this is the maximal set of stable BPS states:

$$\mathcal{S}_{\max} = \left\{(2n,1)_0^{\times 2},\ (2n+1)_{\pm 1},\ (1,0)_{\pm 1}^{\times 2},\ (2,0)_0\right\}\ . \tag{4.5}$$

In the opposite limit, $m\to\infty$, $m\Lambda_2=\Lambda_0^2$ fixed, we expect to flow to the spectrum of the pure gauge theory. To describe this limit conveniently, we should move the cut originating from the massless quark singularity σ_3 to the right so that it disappears in the $m\to\infty$ limit. As explained at the end of Section 2, we can then choose to work with a and $\tilde{a}_D$ instead, which are the quantities that flow to $a^{(0)}$ and $a_D^{(0)}$. We call the corresponding quantum numbers $\tilde{n}_e$, $\tilde{n}_m$ and $\tilde{s}$:

$$n_m=\tilde{n}_m \quad , \quad n_e=\tilde{n}_e+\epsilon\, n_m \quad , \quad s=\tilde{s}+\epsilon\, n_m\ , \tag{4.6}$$

where we recall that $\epsilon=\mathrm{sign}(\Im m\, u)$. Hence, in the $m\to\infty$ limit, we expect to have semiclassically the W-boson $(\tilde{n}_e,\tilde{n}_m)_{\tilde{s}}=(2,0)_0$ as well as the dyons $(\tilde{n}_e,\tilde{n}_m)_{\tilde{s}}=(2k,1)_0$. Converting back to the $(n_e,n_m)_s$ we always use in this paper, these are $(2,0)_0$ as well as the dyons $(2n+1,1)_\epsilon$: only dyons of *odd* n_e and $s=1$ in the upper or $s=-1$ in the lower half plane should survive the RG flow to $N_f=0$ in the weak coupling region. All other states must disappear. There are two possibilities. A state may simply drop out of the spectrum since its BPS mass diverges as $m\to\infty$ as is the case of all states with $\tilde{s}\neq 0$, i.e $s\neq\epsilon\, n_m$. But a state can also disappear at a point u (kept fixed), already at finite m, because it is "hit" by its corresponding decay curve which moves outwards as m is increased. We will see below that this latter possibility is realised for all dyons $(2n,1)_0,\ n\neq 0$, as well as for the the dyons $(2n+1)_{-\epsilon},\ n\neq -1,0$. The remaining undesired states, namely $(0,1)_0,\ (\pm 1,1)_{-\epsilon}$ and $(1,0)_{\pm 1}$ simply disappear because their BPS masses diverge.

4.1. **Possible decay reactions and decay curves**

In this section, we explain how the claim (P) stated in Section 3.2 drastically restricts the number of possible decay reactions and decay curves on which they may occur. We will only use the basis of a and a_D and the corresponding quantum numbers $(n_e,n_m)_s$. Recall that the BPS mass is $M_{\mathrm{BPS}}=\sqrt{2}|n_m a_D-n_e a+s\frac{m}{\sqrt{2}}|$. As discussed above, the maximal set of BPS states then consists of $\mathcal{S}_{\max}$ (as well as their antiparticles). These states also constitute the semi-classical spectrum. Obviously, if at some point $u\in\mathcal{M}$ a BPS state decays into two other states, the latter must be BPS states and must be contained in this maximal spectrum $\mathcal{S}_{\max}$. As in [4] one may also check that matching of the flavour quantum numbers does not give rise to any new constraints: the flavour quantum numbers are related to n_e and s in such a way that they match automatically if n_e and s do. The following results do not depend on whether the bare mass m is larger or smaller than $\frac{\Lambda_2}{2}$. For reasons mentioned at the end of Section 3.1,

we will only need to consider decays into *two* types of BPS states:

$$(n_e, n_m)_s \;\rightarrow\; k \times (n'_e, n'_m)_{s'} + l \times (n''_e, n''_m)_{s''} \;. \tag{4.7}$$

The quantum numbers n'_m, n''_m always are either 0 or 1, since we can always choose $n'_m, n''_m \geq 0$, i.e. a state $(n_e, -1)_s$ is written as $(-1) \times (-n_e, 1)_{-s}$. One has to establish the possible decays of each type of BPS state separately.

As an axample, we present the discussion of all possible decays for the dyons $(2n, 1)_0$. The corresponding decay curves are

$$0 = \Im m \, \frac{n'_m a_D - n'_e a + s' \frac{m}{\sqrt{2}}}{a_D - 2na} \quad \Leftrightarrow \quad 0 = \Im m \, \frac{r_{\rm d} a - \frac{m}{\sqrt{2}}}{a_D - 2na} \quad , \quad r_{\rm d} = \frac{n'_e - 2n n'_m}{s'} \;. \tag{4.8}$$

Either $n'_m = 0$ or $n'_m = 1$. Consider first $n'_m = 0$. Then this is the W-boson or a quark. In the first case we simply have $(2n, 1)_0 \;\rightarrow\; k \times (2, 0)_0 + (2n - 2k, 1)_0$. The value of r for this decay is ∞. In the second case we can have k quarks $(1, 0)_{\pm 1}$ and the dyon $(2n - k, 1)_{s''}$ with $s'' = \mp k$. Hence $|k| = 1$ and we have two possibilities: $(2n, 1)_0 \;\rightarrow\; (1, 0)_{\pm 1} + (2n - 1, 1)_{\mp 1}$ and $(2n, 1)_0 \;\rightarrow\; (-1) \times (1, 0)_{\pm 1} + (2n + 1, 1)_{\pm 1}$ with $r = \pm 1$. Consider now $n'_m = 1$ (and $n''_m = 1$, otherwise we are back to the previous case). Then $(2n, 1)_0 = k \times (n'_e, 1)_{s'} + l \times (n''_e, 1)_{s''}$ implies $l = 1 - k$ and $ks' + (1 - k)s'' = 0$. Since $|s'|, |s''| = 0$ or 1 this implies $s' = s'' = 0$ (since the cases $k = 0$ or $k = 1$, i.e. $l = 0$ must be excluded because they do not give decays). Hence n'_e and n''_e are even and $n = kn'_e + (1 - k)n''_e$. Finally we get $(2n, 1)_0 \;\rightarrow\; k \times (2p, 1)_0 + (1 - k) \times (2q, 1)_0$ with $n = kp + (1 - k)q$ with $r = \infty$ again.

We have determined the possible decays for all the other states, namely the W-boson $(2, 0)_0$, the dyons $(2n + 1, 1)_{\pm 1}$ and the quarks $(1, 0)_{\pm 1}$ in exactly the same way. The results are collected in Table 1. This Table also shows the equations that determine the curves corresponding to the decays.

As already noted above and as will be discussed in detail below, not all curves are relevant. It will turn out that the only relevant curves are

$$\mathcal{C}^{\infty} \quad : \quad \Im m \, \frac{a}{\epsilon a_D + \frac{m}{\sqrt{2}}} = 0 \qquad , \qquad \mathcal{C}^{\pm}_n \quad : \quad \Im m \, \frac{a \pm \frac{m}{\sqrt{2}}}{a_D - na} = 0 \;. \tag{4.9}$$

4.2. **Decay curves and BPS spectra for small mass ($m < \frac{\Lambda_2}{2}$)**

The general picture

We are now ready to establish the exact existence domains for every BPS state. In this subsection, we will discuss the case of small mass, i.e. $m < \frac{\Lambda_2}{2}$. Although it is not too much different, it is more convenient to discuss the case of $m > \frac{\Lambda_2}{2}$ separately in the next subsection. We will consider each type of BPS state separately. We have seen that for the W-boson and

Table 1:

initial state	decay products	
$---$	$---$	$---$
W $-$ boson $(2,0)_0$	$(1,0)_1+(1,0)_{-1}$	$r_{\rm w}=0$
$\Im m\,\frac{r_{\rm w}a_D+\frac{m}{\sqrt{2}}}{a}=0$	$(2p+2,1)_0+(-1)\times(2p,1)_0$	$r_{\rm w}=\infty$
$r_{\rm w}=n'_m/s'$	$(2p+1,1)_{\pm1}+(-1)\times(2p-1,1)_{\pm1}$	$r_{\rm w}=\pm1$
$---$	$---$	$---$
quarks $(1,0)_{\pm1}$	$(2,0)_0+(-1)\times(1,0)_{\mp1}$	$r_{\rm q}=0$
$\Im m\,\frac{r_{\rm q}a_D+\frac{m}{\sqrt{2}}}{-a\pm\frac{m}{\sqrt{2}}}=0$	$(2p,1)_0+(-1)\times(2p-1,1)_{\mp1}$	$r_{\rm q}=\mp\frac{1}{2p}$
$r_{\rm q}=n'_m/(s'\mp n'_e)$	$(2p+1,1)_{\pm1}+(-1)\times(2p,1)_0$	$r_{\rm q}=\mp\frac{1}{2p}$
$---$	$---$	$---$
dyons $(2n,1)_0$	$k\times(2,0)_0+(2n-2k,1)_0$	$r_{\rm d}=\infty$
	$(1,0)_{\pm1}+(2n-1,1)_{\mp1}$	$r_{\rm d}=\pm1$
$\Im m\,\frac{r_{\rm d}a-\frac{m}{\sqrt{2}}}{a_D-2na}=0$	$(-1)\times(1,0)_{\pm1}+(2n+1,1)_{\pm1}$	$r_{\rm d}=\pm1$
	$k\times(2p,1)_0+(1-k)\times(2q,1)_0$	
$r_{\rm d}=(n'_e-n_en'_m)/s'$	with $n=kp+(1-k)q$	$r_{\rm d}=\infty$
$---$	$---$	$---$
dyons $(2n+1,1)_{\pm1}$	$k\times(2,0)_0+(2n-2k+1,1)_{\pm1}$	$r_{\rm d}=\infty$
	$(1,0)_{\pm1}+(2n,1)_0$	$r_{\rm d}=\pm1$
$\Im m\,\frac{r_{\rm d}a-\frac{m}{\sqrt{2}}}{a_D-(2n+1)a\pm\frac{m}{\sqrt{2}}}=0$	$2\times(1,0)_{\pm1}+(2n-1,1)_{\mp1}$	$r_{\rm d}=\pm1$
	$(-1)\times(1,0)_{\mp1}+(2n+2,1)_0$	$r_{\rm d}=\mp1$
$r_{\rm d}=\frac{n'_e-n_en'_m}{s'-sn'_m}$	$(-2)\times(1,0)_{\mp1}+(2n+3,1)_{\mp1}$	$r_{\rm d}=\mp1$
	$(-1)\times(4p-2n-1,1)_{\mp1}+2\times(2p,1)_0$	$r_{\rm d}=\pm(2n-2p+1)$
	$k\times(2p+1,1)_{\pm1}+(1-k)\times(2q+1,1)_{\pm1}$	
	with $kp+(1-k)q=n$	$r_{\rm d}=\infty$

the dyons $(2n,1)_0$ we only need to consider three curves*: $r=\pm1,\ \infty$. For the quarks and the dyons $(2n+1,1)_{\pm1}$ we have a priori infinitely many possible decay curves ($p\in\mathbf{Z}$), but it

$\star$ The curve $r=0$ for the W-boson or for the quarks is simply $\Im m\,a=0$ which is the half-line $[\sigma_3,\infty)$. Since all states exist in the semiclassical region $u\to\infty$ in the upper and in the lower half plane, every point in $\mathcal{M}$ can be reached from this region without crossing $[\sigma_3,\infty)$. Thus the $\Im m\,a=0$ curve is irrelevant.

is clear that only a few values of p will correspond to kinematically possible decays: although $\frac{Z'}{Z} \in \mathbf{R}$ for all p, only for a few p we will have the additional condition (3.6) that $0 \leq \frac{k\,Z'}{Z} \leq 1$. We have computed all curves numerically using Mathematica. Their exact shape of course depends on the value of m/Λ_2, but is not of much importance. Only their positions relative to each other and to the singularities actually matter and there is no qualitative change as long as $m < \frac{\Lambda_2}{2}$. To check whether a given curve is relevant, i.e. whether $0 \leq \frac{k\,Z'}{Z} \leq 1$ so that the decay is kinematically possible and can really happen, it is enough to proceed as follows: if at *some* point on the curve the decay is kinematically impossible (which can be easily checked by computing Z' and Z numerically at this point) one can always transport the BPS state through the curve at this point where it cannot decay, and thus the curve is irrelevant.† On the other hand, to show that a curve is relevant we must make sure that the decay is possible at any point of the curve. Since the real-valued function $\frac{k\,Z'}{Z}$ varies smoothly along the curve, it is easy to see which real interval is its image and whether it is entirely contained within $[0, 1]$.

Let us already present the results of the analysis that will be given below. We have assembled all the *relevant* decay curves into Fig. 4 that sketches their relative positions and indicates the BPS states that decay across these curves. All curves go through σ_3, while the other intersection point with the real axis depends on the curve: $\sigma_2,\ \sigma_1$ and the points $x_{2n},\ n = 1, 2, \ldots$

There are several types of states: first, we have the states that become massless at the singularities. These are $(0, 1)_0$ and, due to the cuts described differently in the two half planes, $(0, 1)_0$ and $(-1, 1)_{\pm 1}$ in the upper, and $(0, 1)_0$ and $(1, 1)_{\pm 1}$ in the lower half plane. These states exist everywhere (throughout the corresponding half plane).

Second, we have the other dyons of $n_e = \pm 1$, the quarks and the W-boson. These states decay on curves in the inner, strong coupling region of the Coulomb branch of moduli space: The W-boson decays on $\mathcal{C}^\infty$, the quark $(1, 0)_{-1}$ on $\mathcal{C}_0^+$ and the quark $(1, 0)_1$ on the innermost curve $\mathcal{C}_0^-$, while the dyons $(\epsilon, 1)_{-\epsilon}$ decay on $\mathcal{C}_0^+$ and the dyons $(\epsilon, 1)_\epsilon$ on $\mathcal{C}_0^-$.

Third, we have the dyons with $|n_e| \geq 2$. As discussed above, among these one must distinguish two sorts: those that will survive the RG flow $m \to \infty$ to the pure gauge theory and those that do not. The dyons that will survive this RG flow are $(2n + 1, 1)_1$ in the upper half plane and $(2n + 1, 1)_{-1}$ in the lower half plane. These dyons $(n \neq -1, 0)$ all decay on the curve $\mathcal{C}^\infty$ which thus plays a priviledged role. The other dyons, namely $(2n, 1)_0$ $(n \neq 0)$ and $(2n + 1, 1)_{-1}$ in the upper and $(2n + 1, 1)_1$ in the in the lower half plane $(n \neq -1, 0)$ decay on curves $\mathcal{C}_{2k}^\pm,\ k \neq 0$ (where $|2k|$ equals $|n_e|$, $|n_e| + 1$ or $|n_e| - 1$). There are only two states that decay on each of these curves $\mathcal{C}_{2k}^\pm,\ k \neq 0$. These curves move more and more outwards as m is increased. Also, as $|k|$ gets bigger (i.e. the $|n_e|$ of the corresponding dyons increase) these curves more and more reach out towards the semiclassical region. Conversely, as $m \to 0$, all curves flow towards a single curve, say $\mathcal{C}^\infty$.

† Here we actually use the fact that the family of curves for a *given* state is such that the curves do not cross each other, except possibly on the real axis. Note that we always consider the parts of a curve in the lower and upper half plane separately.

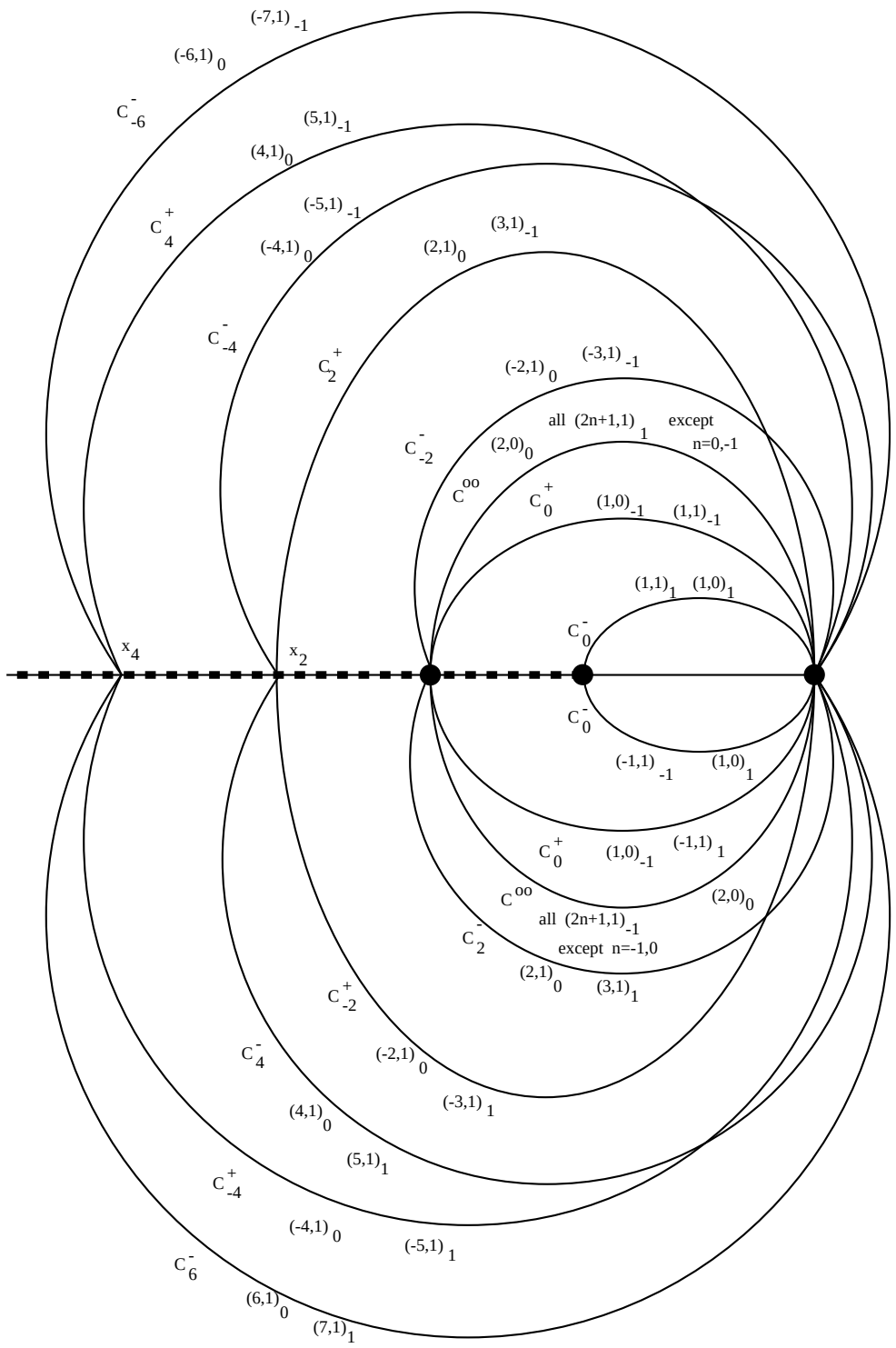

Fig. 4: Shown are a sketch of the relative positions of the relevant decay curves for $m < \frac{\Lambda_2}{2}$ (for not too large $|n_e|$) as well as the BPS states that decay across these curves. Three states do not decay anywhere and still are present in the innermost region inside $\mathcal{C}_0^-$. They are described as $(0,1)_0$ and $(-1,1)_{\pm 1}$ in the upper, and as $(0,1)_0$ and $(1,1)_{\pm 1}$ in the lower half plane. Note that, in reality, the angles at which the curves meet the real axis at the points x_k are slightly different from what they appear to be in the Figure: indeed, the curves $\mathcal{C}^-_{-k-2}$, resp. $\mathcal{C}^+_k$, in the upper half plane are the smooth continuations of the curves $\mathcal{C}^+_{-k}$, resp. $\mathcal{C}^-_{k+2}$, in the lower half plane, in agreement with the monodromy around infinity.

There are a couple of other points worth mentioning. First remark, that the whole picture is compatible with the CP transformation $(n_e, n_m)_s \to (-n_e, n_m)_{-s}$ under reflection by the real u-axis. Second, since all curves go through the singularity σ_3, i.e. all existence domains touch σ_3, it follows that at this point all BPS states exist. The same is true for the points u that lie on the part of the real u line to the right of σ_3. Indeed, as $|n_e|$ is increased, the corresponding dyon curves leaving σ_3 to the right with an ever smaller slope get closer and closer to any given point on the real interval (σ_3, ∞) but never touch it.

Finally we note that the whole picture is perfectly consistent: if a BPS state decays across a given curve, the decay products are also BPS states that must exist in the region considered, i.e. on both sides of the curve. Indeed, this is always the case. As an example, consider the dyons $(2n, 1)_0$ $(n \geq 1)$. In the upper half plane they decay on the curves $\mathcal{C}^+_{2n}$ into the dyons $(2n-1, 1)_1$ and the quark $(1, 0)_{-1}$. These dyons $(2n-1, 1)_1$ exist everywhere in the upper half plane outside $\mathcal{C}^\infty$, while the quark $(1, 0)_{-1}$ exists everywhere outside $\mathcal{C}^+_0$, and in particular in the vicinity of the decay curves of $(2n, 1)_0$ considered. Moreover, in many cases we perform several additional consistency checks to confirm the existence domains we determined.

Now let us prove that our general picture we just described is indeed true. We begin by studying the W-boson.

The W-boson

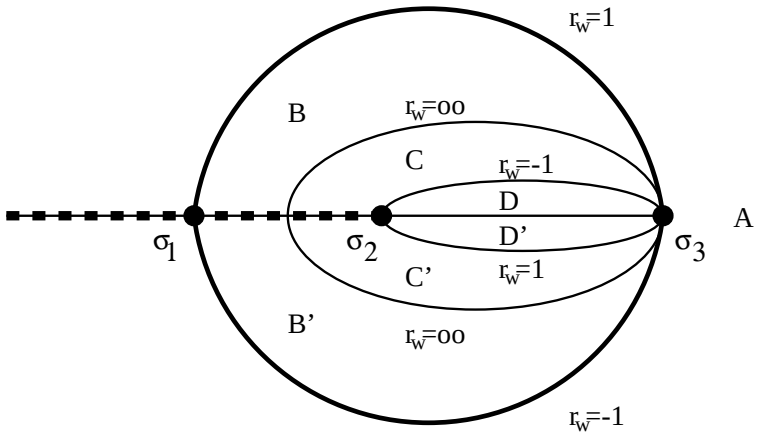

Fig. 5: Sketch of the possible decay curves of the W-boson $(2, 0)_0$ for $m < \frac{\Lambda_2}{2}$. The thick curves $r_{\rm w} = 1$ in the upper half plane and $r_{\rm w} = -1$ in the lower half plane are the only ones that turn out to be relevant: they are $\mathcal{C}^\infty$.

From Table 1 we see that the a priori possible decays are into a dyon and an anti-dyon. The three curves $\Im m \, \frac{r_{\rm w} a_D + \frac{m}{\sqrt{2}}}{a} = 0$ with $r_{\rm w} = \pm 1, \infty$ are shown in Fig. 5.

First consider the curve $r_{\rm w} = \infty$. On this curve a_D/a is real and varies from -1 to 0 in the upper half plane $(\epsilon > 0)$ and from 0 to $+1$ in the lower half plane $(\epsilon < 0)$. It is then easy to see that the only kinematically allowed decays are $(2, 0)_0 \to (0, 1)_0 + (-1) \times (-2, 1)_0$ for $\epsilon > 0$ and $(2, 0)_0 \to (2, 1)_0 + (-1) \times (0, 1)_0$ for $\epsilon < 0$. On the $r_{\rm w} = +1$ curve we similarly

find that the kinematically possible decays are $(2,0)_0 \to (1,1)_1 + (-1)\times(-1,1)_1$ and on the $r_{\rm w} = -1$ curve $(2,0)_0 \to (1,1)_{-1} + (-1)\times(-1,1)_{-1}$ for both $\epsilon > 0$ and $\epsilon < 0$.

Of course, as already mentioned above, such decays can only take place if the final states do indeed exist on the curve considered. This will be checked below for the decay on $\mathcal{C}^\infty$, but for the moment we invite the reader to consult the complete Figure 4 to convince herself/himself that this is indeed the case. We know that the W-boson exists in region A (connected to the semiclassical domain). Also we know that in the $m \to 0$ limit σ_2 coincides with σ_1 and all curves become one and the same curve going through $\sigma_1 = \sigma_2$ and σ_3. From [4] we then know that the W-boson does not exist inside this single $m = 0$ curve. By the RG flow to finite m it is then clear that it does not exist in the innermost regions D and D'. We will now show that the W-boson cannot exist in regions B, B', C or C' either.

Suppose that $(2,0)_0$ exists in region B. Then we can transport it through the cut to region B' without crossing any decay curve. There it would be described* by $(M^*_{2\cdot 3})^{-1}(2,0)_0 = (0,2)_{-2}$. Note that the state $(0,2)_{-2}$ is different from $(2,0)_0$ and would have its own decay curves. We do not say that $(0,2)_{-2}$ would exist in all of region B', but at least it would exist in a region just below the cut that separates B and B'. But such a state with $n_m = 2$ should not exist anywhere on $\mathcal{M}$, hence $(2,0)_0$ cannot exist in B. Suppose now $(2,0)_0$ exists in B'. Then transport it through the cut into region B where it is described as $M^*_{2\cdot 3}(2,0)_0 = (0,-2)_{-2}$ which again does not exist. Exactly the same argument applies for regions C and C'. Independently of the above RG-flow argument, one can see similarly that $(2,0)_0$ cannot exist in D or D'. If it would, there would be a $(M^*_3)^{\mp 1}(2,0)_0 = (2,\pm 4)_0$ in D' or D. We conclude that $(2,0)_0$ cannot exist in any of the regions B, B', C, C', D and D'. Hence it is the $r_{\rm w} = 1$ curve for $\epsilon > 0$ and the $r_{\rm w} = -1$ curve for $\epsilon < 0$ that border the existence domain of the W-boson. These are the two halves of the $\mathcal{C}^\infty$ curve as defined in (4.9). In this sense, $\mathcal{C}^\infty$ is the only relevant curve for this BPS state.

Note that $M_{2\cdot 3}$ acts on (n_e, n_m) as $S \in {\rm SL}(2,\mathbf{Z})$, i.e. it exchanges n_e and n_m (up to a sign). Thus whenever we have a state with $|n_e| \geq 2$ it cannot exist in a region that is bounded by part of the cut $[\sigma_1, \sigma_2]$ (as are regions B, B', C and C' for the W-boson) since this state would be described on the other side of the cut by a $|n_m| \geq 2$. This is a very useful fact which we will employ much in the following.

The quark $(1,0)_1$

From Table 1 we see that there is an infinity of a priori possible decays on the infinite set of curves labelled by $r_{\rm q} = -\frac{1}{2p}$, including $r_{\rm q} = \infty$ for $p = 0$, as indicated in Fig 6.

One easily checks that for all curves with $p \neq 0$ the decays are kinematically impossible. For $p = 0$, however, $(1,0)_1 \to (0,1)_0 + (-1)\times(-1,1)_{-1}$ is kinematically possible for $\epsilon > 0$ while for $\epsilon < 0$ it is $(1,0)_1 \to (-1)\times(0,1)_0 + (1,1)_1$. Note that in both cases the quark decays into

---

$\star$ For typographical convenience we write $M^*(n_e, n_m)_s$ instead of $M^* \begin{pmatrix} n_e \\ n_m \\ s \end{pmatrix}$.

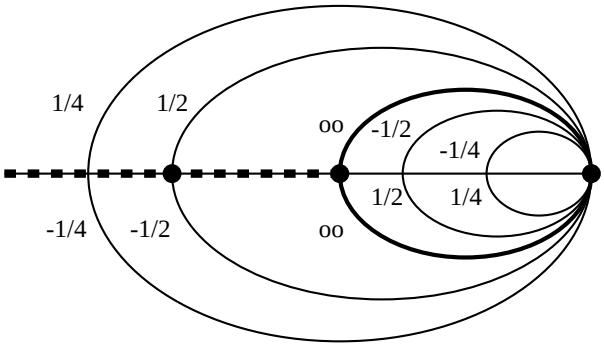

Fig. 6: Sketch of the possible decay curves of the quark $(1,0)_1$ for $m < \frac{\Lambda_2}{2}$ labelled by the values of $r_{\rm q}$. The thick curve $r_{\rm q} = \infty$ is $\mathcal{C}_0^-$ and is the only curve that turns out to be relevant.

the two BPS states that become massless at the singularities σ_2 and σ_3, cf. Fig. 2, and hence indeed exist throughout the corresponding half planes, as we will see below. It is now clear that $(1,0)_1$ exists everywhere outside the $r_{\rm q} = \infty$ curve which is nothing else than the curve $\mathcal{C}_0^-$ as defined in eq. (4.9), while it cannot exist inside, as one sees either from the RG-flow argument or otherwise since one would get states $(M_3^*)^{\pm 1}(1,0)_1 = (1, \mp 2)_1$ with $|n_m| = 2$ that do not exist.

The quark $(1,0)_{-1}$

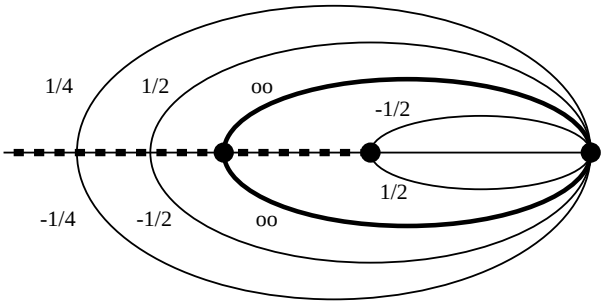

Fig. 7: Sketch of the possible decay curves of the quark $(1,0)_{-1}$ for $m < \frac{\Lambda_2}{2}$ labelled by the values of $r_{\rm q}$. The thick curve $r_{\rm q} = \infty$ is $\mathcal{C}_0^+$ and is the only curve that turns out to be relevant.

Again, there is an infinity of a priori possible decays on the infinite set of curves labelled by $r_{\rm q} = \frac{1}{2p}$, see Fig. 7.

We find again that all decays are kinematically impossible, except for $p = 0$ on the $r_{\rm q} = \infty$ curve: $(1,0)_{-1} \to (0,1)_0 + (-1) \times (-1,1)_1$ for $\epsilon > 0$ and $(1,0)_{-1} \to (-1) \times (0,1)_0 + (1,1)_{-1}$ for $\epsilon < 0$. Note again that the relevant curve goes through σ_1 and σ_3 and that the decay is precisely into the states that are massless at σ_1 and σ_3, cf. Fig 2. Thus we see that the quark $(1,0)_{-1}$ exists everywhere outside the $r_{\rm q} = \infty$ curve and does not exist inside this curve. The

latter fact follows once more from the RG-flow from $m = 0$ or using $(M_3^*)^{\pm 1}$ which would generate a state with $|n_m| = 2$ that does not exist. Note that here the $r_{\rm q} = \infty$ curve is $\mathcal{C}_0^+$ which is different from the relevant decay curve $\mathcal{C}^\infty$ for the W-boson (see eq. (4.9)) although both curves go through σ_1 and σ_3: $\mathcal{C}_0^+$ lies inside $\mathcal{C}^\infty$.

The magnetic monopole $(0,1)_0$

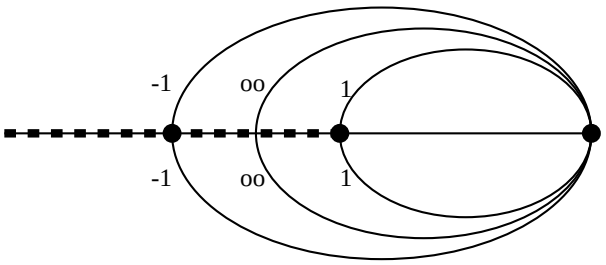

Fig. 8: Sketch of the possible decay curves of the magnetic monopole $(0,1)_0$ for $m < \frac{\Lambda_2}{2}$ labelled by the values of $r_{\rm d}$.

As for all dyons with even n_e, there are only three possible decay curves: $r = \pm 1$ and ∞. For the magnetic monopole, which is massless at σ_3 these three curves are as shown in Fig. 8.

All curves go through σ_3. Hence any point u can be reached by a path that starts at σ_3 and does not cross any curve. Since the monopole certainly exists at σ_3, we conclude that it must exist everywhere. As a consistency check, one can verify that after transporting it through any of the cuts it is decribed by quantum numbers that still correspond to allowed BPS states that indeed do exist there.

The dyons $(2n,1)_0$ with $n \neq 0$

Let first $2n \geq 4$. For all these dyons the three curves $r_{\rm d} = \pm 1$ and ∞ are as sketched in Fig. 9.

In each half plane there are only two curves. The $r = \infty$ curves are the same for all n, while the $r_{\rm d} = 1$ curve in the lower half plane starts at the point x_{2n-2} on the real axis where the $r_{\rm d} = -1$ curve in the upper half plane of the dyon $(2n-2,1)_0$ had ended. In particular, x_{2n} increases as $n(>0)$ is increased. Since the regions B_n, B'_n, C_n and C'_n all are bounded by a portion of the cut $[\sigma_1, \sigma_2]$, by the argument given at the end of the subsection on the W-boson, the dyons $(2n,1)_0$ having $|n_e| \geq 2$, cannot exist in either of these regions: they can only exist in regions A_n. The decay on the $r_{\rm d} = -1$ curve (which is $\mathcal{C}_{2n}^+$) is $(2n,1)_0 \to (1,0)_{-1} + (2n-1,1)_1$ while the decay on the $r_{\rm d} = 1$ curve (which is $\mathcal{C}_{2n}^-$) is $(2n,1)_0 \to (1,0)_1 + (2n-1,1)_{-1}$. We will see below that $(2n-1,1)_1$, resp. $(2n-1,1)_{-1}$ decay on curves that are inside the curves $\mathcal{C}_{2n}^+$, resp. $\mathcal{C}_{2n}^-$, so that the final states of the decays of $(2n,1)_0$ indeed exist. Note the following consistency check: if we transport the dyon $(2n,1)_0$ from region A_n through the interval $[x_{2n}, x_{2n-2}]$ into the upper half plane, it is described on the other side of the cut as $M^*_{1\cdot 2\cdot 3}(2n,1)_0 = (2-2n,-1)_0 = -(2n-2,1)_0$ which indeed does exist in the region above $[x_{2n}, x_{2n-2}]$.

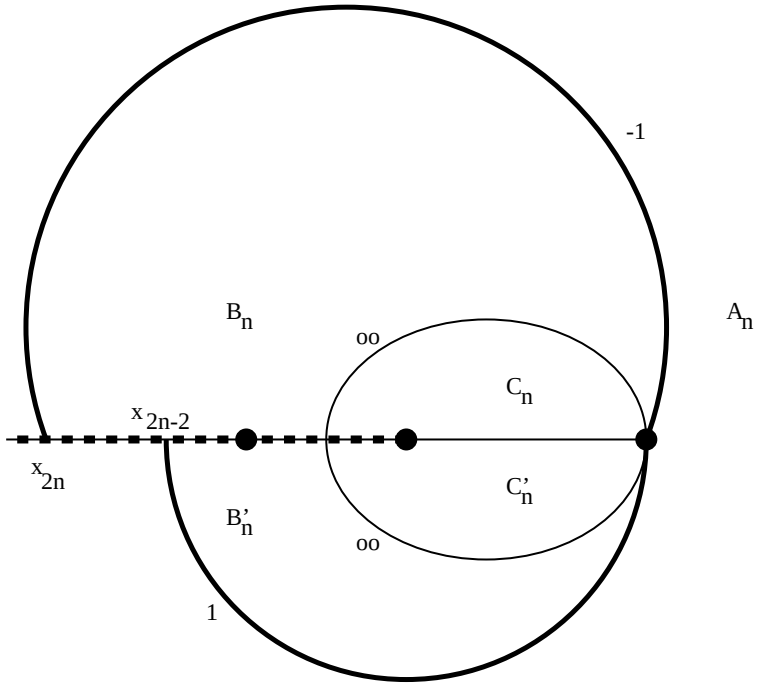

Fig. 9: Sketch of the possible decay curves of the dyons $(2n,1)_0$, $2n \geq 4$, for $m < \frac{\Lambda_2}{2}$ labelled by the values of $r_{\rm d}$. The thick curves are those that turn out to be relevant. They are $\mathcal{C}^+_{2n}$ in the upper half plane and $\mathcal{C}^-_{2n}$ in the lower half plane.

Now consider the dyon $(2,1)_0$, i.e. $n=1$. Then the point $x_{2n-2} \equiv x_0$ coincides with the singularity σ_1, but this does not change the general argument just given. What is different however, is the appearence of an additional curve in the lower half plane, namely $r_{\rm d} = -1$ which goes from σ_2 to σ_3 and separates region C'_1 into a region C' and an innermost region D. The above argument that the dyon cannot exist in region C'_n now applies to C'. To show that $(2,1)_0$ cannot exist in D either, it is enough to show that it cannot decay across this $r_{\rm d} = -1$ curve separating C' and D. The only kinematically possible decay on this curve would be $(2,1)_0 \to (1,0)_{-1} + (1,1)_1$. But the quark $(1,0)_{-1}$ does not exist in the neighbourhood on either side of this curve as we have shown above. So $(2,1)_0$ cannot exist in region D either. This also follows from the RG-flow from $m=0$ or by applying M_3^* when crossing the cut, which provides some consistency checks.

Contrary to the other states considered before, the dyons $(2n,1)_0$ with $n \geq 1$ have existence domains that are asymmetric with respect to reflection by the real axis, i.e. under complex conjugation. However this is not surprising: reflection corresponds to CP and for the states considered before, CP only mapped them to their antiparticles which must exist in the same domains. On the other hand, CP maps the dyon $(2n,1)_0$ to $(-2n,1)_0$ which is a different BPS state. CP then tells us that the dyons $(-2n,1)_0$ exist in domains $\overline{A_n}$ that are the complex conjugate of the existence domains A_n of the $(2n,1)_0$. The domains $\overline{A_n}$ are bounded by the curves $\mathcal{C}^-_{-2n} = \overline{\mathcal{C}^-_{2n}}$ in the upper half plane and by $\mathcal{C}^+_{-2n} = \overline{\mathcal{C}^+_{2n}}$ in the lower half plane ($n > 0$).

Next we will turn to the dyons with odd n_e and $s = \pm 1$. Since the dyons $(2n+1,1)_{-1}$ are

the CP conjugates of the dyons $(-2n-1,1)_{+1}$ it is enough to consider the dyons $(2n+1,1)_1$ for all $n \in \mathbf{Z}$. For each of these dyons of odd n_e, there is an infinity of a priori possible decay curves, one for every odd r and one for $r = \infty$.

The dyon $(-1,1)_1$

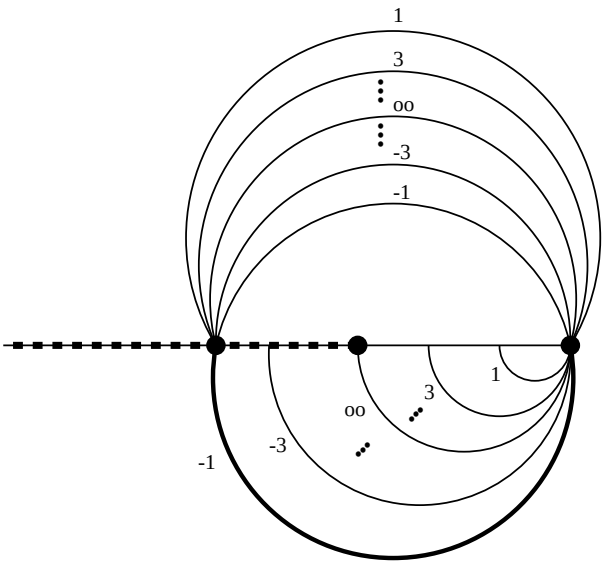

Fig. 10: Sketch of the possible decay curves of the dyon $(-1,1)_1$ for $m < \frac{\Lambda_2}{2}$ labelled by the values of $r_{\rm d}$. The thick curve ($\mathcal{C}_0^+$) is the one that turns out to be relevant.

All curves go through σ_3, and the curves in the upper half plane all end at σ_1 where this dyon is massless. The curves are shown in Fig. 10.

Since the dyon $(-1,1)_1$ exists at σ_1 when approached from the upper half plane, we can always transport it to any point in this half plane without crossing any curve, and thus we know that it exists everywhere in the upper half plane. Let us now focus on the lower half plane. The curves with $r_{\rm d} = -2p-1$ correspond to the decays $(-1,1)_1 \to 2\times(2p,1)_0+(-1)\times(4p+1,1)_{-1}$. Clearly, if $|p|$ is too large, the final states will be too massive and the decay is impossible. We find that on the $r_{\rm d} = -1$ curve ($p = 0$) the decay $(-1,1)_1 \to 2\times(0,1)_0+(-1)\times(1,1)_{-1}$ is indeed possible, i.e. $(-1,1)_1$ decays into the states that are massless at σ_3 and σ_1 in the lower half plane. We also find that no decays are kinematically possible on the $r_{\rm d} = -3,\ -5,\ \ldots$ curves. In any case, $(-1,1)_1$ cannot exist in any of the regions in the lower half plane between two curves $r_{\rm d} = -2p-1$ and $r_{\rm d} = -2p-3$ ($p = 0,\ 1,\ 2,\ \ldots$) because these regions touch part of the cut $[\sigma_1,\sigma_2]$ and hence the existence of $(-1,1)_1$ would imply the existence of $M^*_{2.3}(-1,1)_1 = (1,1)_3$ just above the cut. However, such a state has $s = 3$ and cannot exist. Similarly, $(-1,1)_1$ cannot exist between any of the curves $r_{\rm d} = 2p+1$ and $r_{\rm d} = 2p+3$ ($p = 0,\ 1,\ 2,\ \ldots$) in the lower half plane because they touch part of the cut $[\sigma_2,\sigma_3]$, and we would similarly conclude that a state $M^*_3(-1,1)_1 = (-1,3)_1$ would exist just above the cut. We conclude that the dyon

$(-1,1)_1$ exists everywhere except in the region of the lower half plane that is bounded by the cut $[\sigma_1, \sigma_3]$ and the $r_{\rm d} = -1$ curve which is nothing else than $\mathcal{C}_0^+$ (or actually its part in the lower half plane).

As discussed above, it follows from CP that the dyon $(1,1)_{-1}$ exists everywhere outside the mirror image of the region just described, which is bounded by $[\sigma_1, \sigma_3]$ and the part in the upper half plane of the curve $\mathcal{C}_0^+$.

The dyon $(1,1)_1$

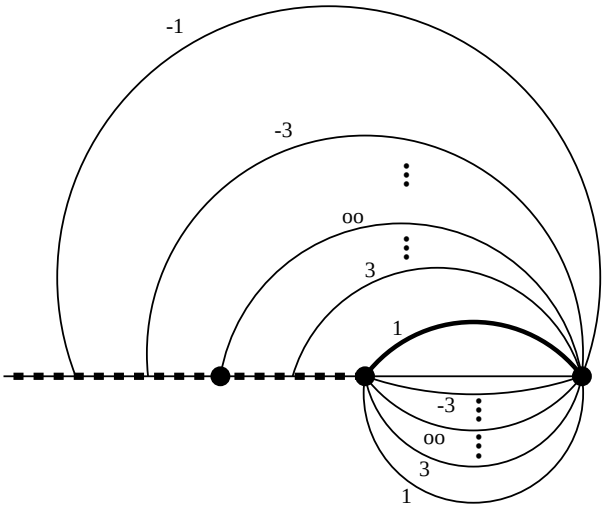

Fig. 11: Sketch of the possible decay curves of the dyon $(1,1)_1$ for $m < \frac{\Lambda_2}{2}$ labelled by the values of $r_{\rm d}$. The thick curve ($\mathcal{C}_0^-$) is the one that turns out to be relevant.

All curves go through σ_3, and the curves in the lower half plane all start at σ_2 where this dyon is massless. They are shown in Fig. 11.

Again, any point in the lower half plane can be reached from σ_2 without crossing any curve, and hence $(1,1)_1$ exists everywhere in the lower half plane. What about the upper half plane? It turns out that there the only curve on which a decay is kinematically possible is the $r_{\rm d} = 1$ curve with the decay $(1,1)_1 \to 2 \times (0,1)_0 + (-1) \times (-1,1)_{-1}$ with the final states being again those BPS states that are massless at σ_3 and σ_2 in the upper half plane. It is then clear that this decay must happen as $(1,1)_1$ cannot exist inside the $r_{\rm d} = 1$ curve. This can be seen either from the RG-flow argument from $m = 0$, or else since the existence of $(1,1)_1$ in this region would imply the existence of $(M_3^*)^{-1}(1,1)_1 = (1,3)_1$ below the cut $[\sigma_2, \sigma_3]$ which is excluded. We conclude that the dyon $(1,1)_1$ exists everywhere outside the region bounded by $[\sigma_2, \sigma_3]$ and the $r_{\rm d} = 1$ curve in the upper half plane which is nothing else than the corresponding part of $\mathcal{C}_0^-$. By CP we see that the dyon $(-1,1)_{-1}$ exists everywhere outside a region bounded by $[\sigma_2, \sigma_3]$ and the part of $\mathcal{C}_0^-$ in the lower half plane.

The dyons $(2n+1,1)_1$ with $n > 0$

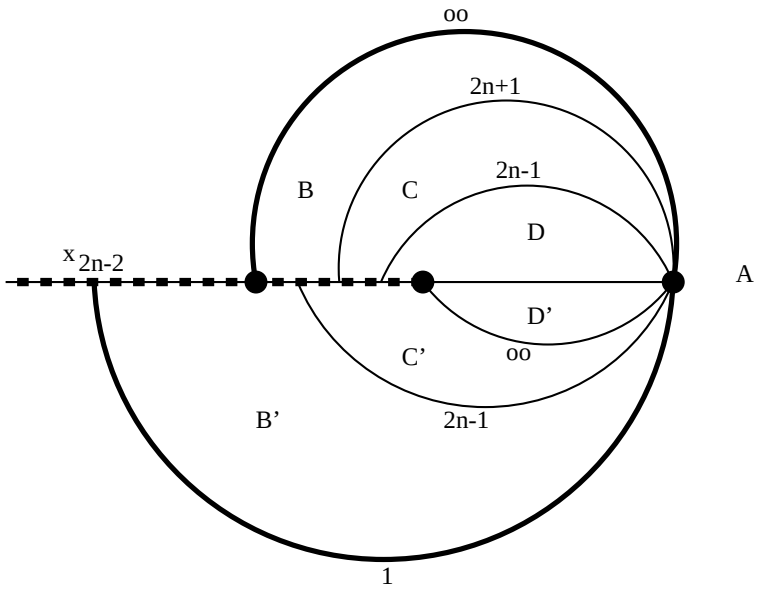

Fig. 12: Sketch of the possible decay curves of the dyons $(2n+1,1)_1$ for $m < \frac{\Lambda_2}{2}$ labelled by the values of $r_{\rm d}$. The thick curves are those that turn out to be relevant. They are $\mathcal{C}^{\infty}$ in the upper half plane and $\mathcal{C}^{-}_{2n}$ in the lower half plane.

Among the infinity of a priori possible decay curves, we find that the decays are kinematically possible only on the following ones: in the upper half plane on $r_{\rm d} = \infty$, $r_{\rm d} = 2n+1$ and $r_{\rm d} = 2n-1$ and in the lower half plane on $r_{\rm d} = \infty$, $r_{\rm d} = 2n-1$ and $r_{\rm d} = 1$. These curves are shown in Fig. 12.

The curves shown in Fig. 12 are generic, except for $2n+1 = 5$ where the $r_{\rm d} = 2n-1 = 3$ curve in the upper half plane ends at σ_2, and for $2n+1 = 3$ where there is no $r_{\rm d} = 2n-1 = 1$ curve in the upper half plane and where the $r_{\rm d} = 2n-1$ curve in the lower half plane coincides with the $r_{\rm d} = 1$ curve and starts at $x_0 \equiv \sigma_1$.

There are two kinematically possible decays on the $r_{\rm d} = 1$ curve: $(2n+1,1)_1 \to (1,0)_1 + (2n,1)_0$ and $(2n+1,1)_1 \to 2\times(1,0)_1 + (2n-1,1)_{-1}$. But this curve is $\mathcal{C}^{-}_{2n}$ and hence also the decay curve of $(2n,1)_0$ (where the latter decays into $(1,0)_1 + (2n-1,1)_{-1}$), so that the first of the two decays cannot take place (or actually is identical to the second). On the other hand, we will see below that $(2n-1,1)_{-1}$ exists in the lower half plane everywhere outside the curve $\mathcal{C}^{\infty}$ which is well inside $\mathcal{C}^{-}_{2n}$ $(n > 0)$, so that the second of the two decays can indeed take place. In the upper half plane, on the $r_{\rm d} = \infty$ curve (which is $\mathcal{C}^{\infty}$) we can have the decay $(2n+1,1)_1 \to (n+1)\times(1,1)_1 + (-n)\times(-1,1)_1$ into final states that do exist there. The existence of $(2n+1,1)_1$ in regions B, C, D, B', C' and D' is ruled out by the by now familiar arguments of transporting the state through the cuts $[\sigma_1,\sigma_2]$ or $[\sigma_2,\sigma_3]$ and thus generating states $(M^*_{2\cdot3})^{\pm1}(2n+1,1)_1$ or $(M^*_3)^{\pm1}(2n+1,1)_1$ that would have $|n_m| \geq 2$.

The dyons $(2n+1,1)_1$ with $n < -1$

The decay curves on which the decays are kinematically possible look qualitatively very much like those of Fig. 12. The only curve that starts in the lower half plane to the left of σ_1

is the curve $\mathcal{C}^+_{2n+2}$ (which is now $r_{\rm d} = -1$ and replaces the $r_{\rm d} = 1$ curve of Fig. 12), while in the upper half plane we still have the same $r = \infty$ curve $\mathcal{C}^\infty$. By the same arguments, using $(M^*_{2\cdot 3})^{\pm 1}$ and $(M^*_3)^{\pm 1}$, we can show that the dyons under consideration only exist outside these two curves. The decay on $\mathcal{C}^\infty$ is e.g. $(2n+1,1)_1 \to (n+1)\times(1,1)_1 + (-n)\times(-1,1)_1$ as before, while on $\mathcal{C}^+_{2n+2}$ it is $(2n+1,1)_1 \to 2\times(-1,0)_1 + (2n+3,1)_{-1}$ which do exist there.

The dyons $(2n+1,1)_{-1}$

These dyons are the CP conjugate states of $(-2n-1,1)_1$. Hence, in the lower half plane they always exist everywhere outside the curve $\mathcal{C}^\infty$, while in the upper half plane they only exist outside curves $\mathcal{C}^+_{2n}$ if $n > 0$ and only outside curves $\mathcal{C}^-_{2n+2}$ if $n < -1$. As a consistency check, consider transporting a dyon $(2n+1,1)_1$ with $n > 0$ through the cut $(-\infty, \sigma_1]$ (see Fig. 12) into the region below the cut. Then this state is described there by $(M^*_{1\cdot 2\cdot 3})^{-1}(2n_1,1)_1 = -(2n+3,1)_{-1}$. This state indeed exists in this region because it is outside $\mathcal{C}^\infty$ (in the lower half plane).

4.3. **Decay curves and BPS spectra for large mass ($m > \frac{\Lambda_2}{2}$)**

The general picture

As m is increased from $m < \frac{\Lambda_2}{2}$ to $m > \frac{\Lambda_2}{2}$ one goes through $m = \frac{\Lambda_2}{2}$ where the singularities σ_2 and σ_3 coincide and where new states become massless. At $m > \frac{\Lambda_2}{2}$, the quantum numbers of the massless states at these two singularities have changed. One must however keep in mind that this is a somewhat "local" effect, where locality here refers to the distance on the Coulomb branch: these rearrangements do not much affect $a(u)$ or $a_D(u)$ for u far away, i.e. such that $|u-\sigma_2| \gg |\sigma_2 - \sigma_3|$. What does this mean for the relevant decay curves and existence domains of the BPS states of Fig. 4? We expect, and verify below, that all what can happen is the following: as $m = \frac{\Lambda_2}{2}$ and $\sigma_2 = \sigma_3$, the curve $\mathcal{C}^-_0$ has shrunk to a point. Then as m is increased beyond $\frac{\Lambda_2}{2}$ and σ_3 moves off to the right, all curves (except $\mathcal{C}^-_0$) remain "attached" to the real axis "at the left" at points σ_1, x_{2n} (that, of course, do move as m is varied), while at their right some curves remain attached at σ_2 while others are attached at σ_3. It turns out that all curves $\mathcal{C}^+_{2n}$, $n \in \mathbf{Z}$ are attached to σ_2, and all curves $\mathcal{C}^-_{2n}$ with $n < 0$ for $\epsilon > 0$ and $n > 0$ for $\epsilon < 0$ are attached to σ_3. But there appears also a new family of relevant curves, attached to σ_2 and σ_3: these are the curves $\mathcal{C}^-_{2n}$ with $n \geq 0$ for $\epsilon > 0$ and $n \leq 0$ for $\epsilon < 0$. All this is shown in Fig. 13. The only states existing inside the $\mathcal{C}^+_0$ curve are the three dyons $(\epsilon,1)_\epsilon$, $(-\epsilon,1)_\epsilon$, $(-\epsilon,1)_{-\epsilon}$ as well as the quark $(1,0)_1$ and the monopole $(0,1)_0$. The dyon $(-\epsilon,1)_{-\epsilon}$ and the monopole $(0,1)_0$ however decay on the curve $\mathcal{C}^-_0$ between σ_2 and σ_3. So, as always, the only BPS states that exist everywhere are the three states that are responsible for the singularities, namely the two dyons $(\pm\epsilon,1)_\epsilon$ and the quark $(1,0)_1$.

Note that, as $m \to \infty$, the special dyons $(-\epsilon,1)_\epsilon$ and $(\epsilon,1)_\epsilon$ have finite masses as do all dyons $(2n+1,1)_\epsilon$ as well as the W-boson. These states thus survive the RG flow to the pure gauge theory. These surviving states all decay on one and the same curve, $\mathcal{C}^\infty$ which one may consider as fixed under the flow (except for $(-\epsilon,1)_\epsilon$ and $(\epsilon,1)_\epsilon$, of course). After transforming to the natural quantum numbers $(\tilde{n}_e, n_m)_{\tilde{s}}$ of the pure gauge theory, see eq. (4.6), we see that

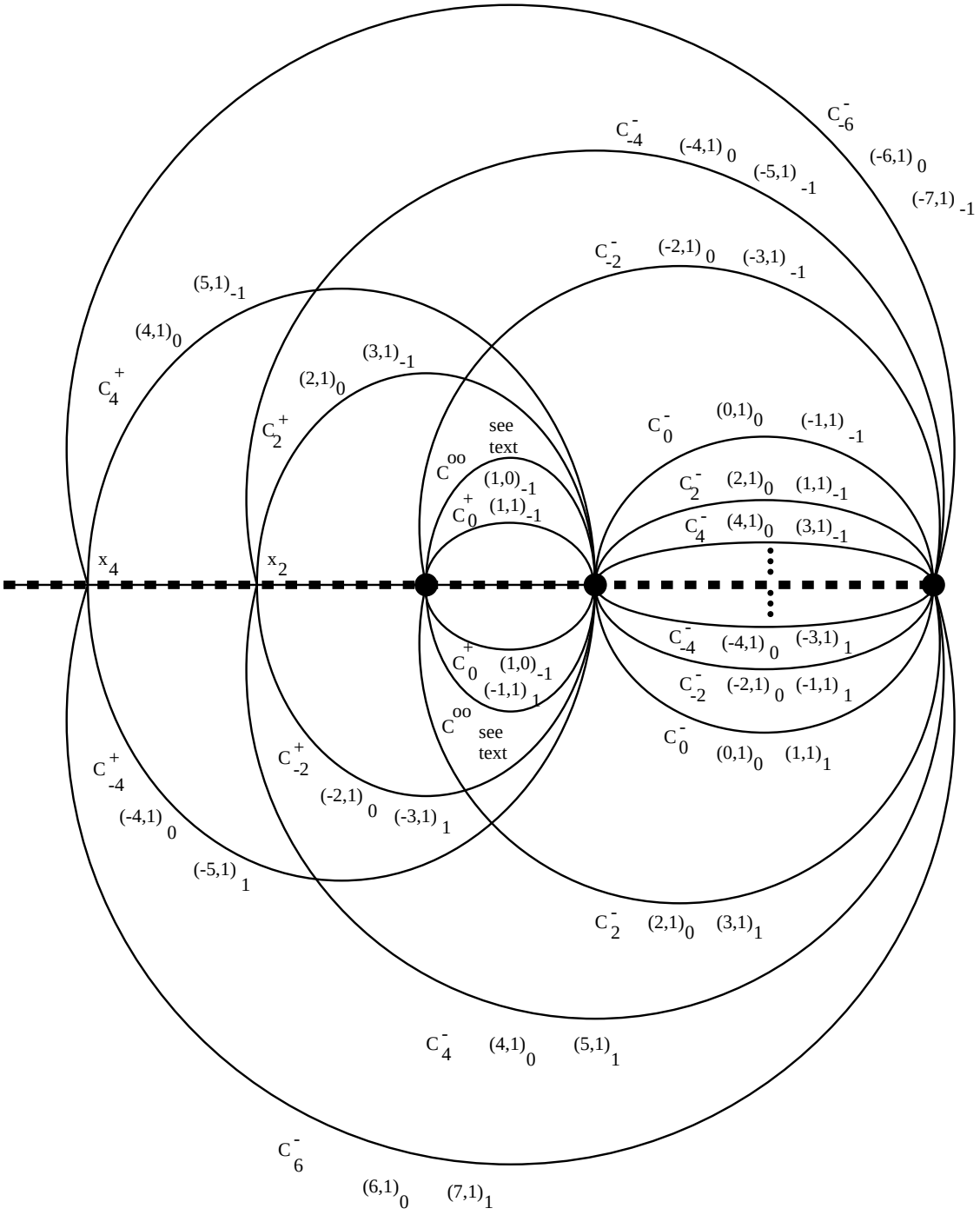

Fig. 13: Shown are a sketch of the relative positions of the relevant decay curves for $m > \frac{\Lambda_2}{2}$ as well as the BPS states that decay across these curves (for not too large $|n_e|$). The BPS states that decay across $\mathcal{C}^\infty$ in the upper half plane are the W-boson $(2,0)_0$ as well as all dyons $(2n+1,1)_1,\ n \neq -1,0$, while the states decaying across $\mathcal{C}^\infty$ in the lower half plane are again the W-boson $(2,0)_0$ as well as all dyons $(2n+1,1)_{-1},\ n \neq -1,0$. The only states existing inside the $\mathcal{C}_0^+$ curve are the three dyons $(\epsilon,1)_\epsilon$, $(-\epsilon,1)_\epsilon$, $(-\epsilon,1)_{-\epsilon}$ as well as the quark $(1,0)_1$ and the monopole $(0,1)_0$.

these states all have $\tilde{s} = 0$ and precisely constitute the spectrum of the pure gauge theory as established in [3]. On the other hand, the states that do not survive this flow either simply disappear from the spectrum because their masses diverge, as is the case of the quarks or the special dyons $(\pm 1, 1)_{-\epsilon}$ or $(0, 1)_0$ inside $\mathcal{C}^\infty$, or because they are "hit" by their decay curve that moves outwards as $m \to \infty$. Indeed, any point u which for some m still is in the existence domain of a given BPS state will be hit by the corresponding curve for large enough m. Note that again, as for $m < \frac{\Lambda_2}{2}$, all BPS states exist at σ_3 and in a narraow wedge extending to the right of it, in particular on the real interval $[\sigma_3, \infty)$. Of course, this does not prevent any real point u to be hit by the curves: As $m \to \infty$ we also have $\sigma_3 \to \infty$ and any point u will eventually end up inside the curves.

Now let us briefly comment on the discrepancy with the published version of [9]. The authors of [9], for $N_f = 2$ with equal bare masses, consider a real point u to the *right* of the singularity σ_3 and write that a certain dyon does no longer exist there for a certain mass $m > \frac{\Lambda_2}{2}$. In the light of what we have said so far, it is clear that this cannot be true. This fact is even more obvious since, if it were true, we would need to have decay curves crossing the real u axis to the right of σ_3 where there are no cuts - a situation that cannot occur as one can easily see, also without our detailed analysis. The authors of [9] have checked this point again, and told us that they actually agree with our result, the discrepancy being only due to some error when writing up their paper.

In the remainder of this subsection, we will again discuss the decay curves for each type of BPS state, thus proving Fig. 13 to be correct.

The dyons $(2n, 1)_0$

Recall that decays can only happen on the curves (4.8) for $r = \pm 1$ and ∞. But numerically we find that the $r_{\rm d} = \infty$ curve has disappeared. Actually, as m approaches $\frac{\Lambda_2}{2}$ from below, one can see how this curve (which goes through σ_3, see Figs. 8 to 9) shrinks to a point, and its absence at $m > \frac{\Lambda_2}{2}$ is perfectly compatible with a smooth RG flow as m is increased.

For a generic dyon $(2n, 1)_0$ with $n \geq 2$ one finds for the $r_{\rm d} = \pm 1$ curves the situation depicted in Fig. 14 on the left. The $r_{\rm d} = 1$ curve (for $\epsilon > 0$ and $\epsilon < 0$) is the curve $\mathcal{C}^-_{2n}$ while the $r_{\rm d} = -1$ curve ($\epsilon > 0$) is $\mathcal{C}^+_{2n}$. All curves turn out to be relevant with the following kinematically possible decays: $(2n, 1)_0 \to (1, 0)_{-1} + (2n-1, 1)_1$ on $r_{\rm d} = -1$, $(2n, 1)_0 \to (-1) \times (1, 0)_1 + (2n+1, 1)_1$ on $r_{\rm d} = 1$ for $\epsilon > 0$ and $(2n, 1)_0 \to (1, 0)_1 + (2n-1, 1)_{-1}$ on $r_{\rm d} = 1$ for $\epsilon < 0$. To show that $(2n, 1)_0$ cannot exist in regions C_n, B_n and B'_n we use the same type of argument as before. The monodromy $M_{2\cdot 3}$ around σ_2 and σ_3 is the same as for small mass, and just as before, transporting the dyon $(2n, 1)_0$ from C_n to B'_n through the cut $[\sigma_1, \sigma_2]$ or vice versa would result in states with $|n_m| = 2n$ that cannot exist. To prove the non-existence of $(2n, 1)_0$ in B_n, transport it to B'_n where it is described as $(M_3^*)^{-1}(2n, 1)_0 = (2n-2, 1)_{-2}$ which has $s = -2$ and cannot exist. We conclude that $(2n, 1)_0$ only exists in regions A_n outside these curves. The only difference for $n = 1$, i.e. for the dyon $(2, 1)_0$ is that the point $x_{2n-2} \equiv x_0$ coincides with σ_1, but this does not change the preceeding discussion.

The dyons $(2n, 1)_0$ with $n < 0$ are the CP conjugates of the dyons $(-2n, 1)_0$ with $-2n > 0$, and thus exist in the complex conjugate domains $A_n = \overline{A_{-n}}$.

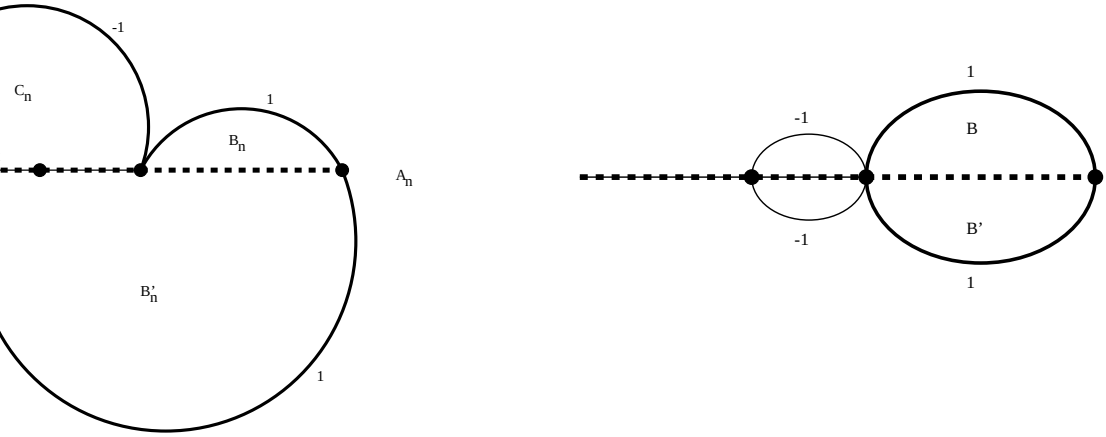

Fig. 14: In the left figure we show a sketch of the relative positions of the decay curves of the dyons $(2n,1)_0$ $(n>1)$ for $m > \frac{\Lambda_2}{2}$. All curves shown are relevant. The figure on the right shows a sketch of the relative positions of the decay curves of the monopole $(0,1)_0$. The thick curves are the relevant ones.

The situation is slightly different for the monopole $(0,1)_0$, as shown in Fig. 14 on the right. No decays are possible on the $r=-1$ curve while on the $r=1$ curve one has $(0,1)_0 \to (-1)\times(1,0)_1 + (1,1)_1$ for $\epsilon > 0$ and $(0,1)_0 \to (1,0)_1 + (-1,1)_{-1}$ for $\epsilon < 0$. The monopole cannot exist in B or B' since this would lead to $(M_3^*)^{\pm 1}(0,1)_0 = (\pm 2,1)_{\pm 2}$ on the other side of $[\sigma_2,\sigma_3]$ which, having $|s|=2$, is excluded.

The dyons $(2n+1,1)_1$

Fig. 15: Shown is a sketch of the relative positions, for $m > \frac{\Lambda_2}{2}$, of the decay curves of the dyon $(1,1)_1$ (left) and of the dyon $(-1,1)_1$ (right). The thick curves are the relevant ones.

First, look at the dyon $(1,1)_1$ for which the curves are as shown in the left Fig. 15. All curves go through σ_2 where this dyon is massless when approached from $\epsilon > 0$, and we see that it must exist in the whole upper half plane. It cannot exist in region B' since otherwise

this would imply the existence of $M_3^*(1,1)_1 = (3,1)_3$ above the cut. Note that conversely, the existence of $(1,1)_1$ in B only implies the existence of $(M_3^*)^{-1}(1,1)_1 = (-1,1)_{-1}$ below the cut which is perfectly consistent (see Fig 13). The decay across the $r_{\rm d} = 1$ curve for $\epsilon < 0$ ($\mathcal{C}_0^-$) is $(1,1)_1 \to 2 \times (1,0)_1 + (-1,1)_{-1}$ into final states that are massless in the lower half plane at σ_3 and σ_2.

Next, consider the dyon $(-1,1)_1$ with curves shown in the right Fig. 15. All curves in the upper half plane go through σ_1 where this dyon is massless. Hence it exists everywhere in the upper half plane. It cannot exist in B or in C since $M_{2\cdot3}^*(-1,1)_1 = (1,1)_3$ and $M_3^*(-1,1)_1 = (1,1)_3$. The decays in the lower half plane are $(-1,1)_1 \to (-1) \times (1,0)_{-1} + (0,1)_0$ on $r_{\rm d} = -1$ ($\mathcal{C}_0^+$) and $(-1,1)_1 \to 2 \times (1,0)_1 + (-3,1)_{-1}$ on $r_{\rm d} = 1$ ($\mathcal{C}_{-2}^-$).

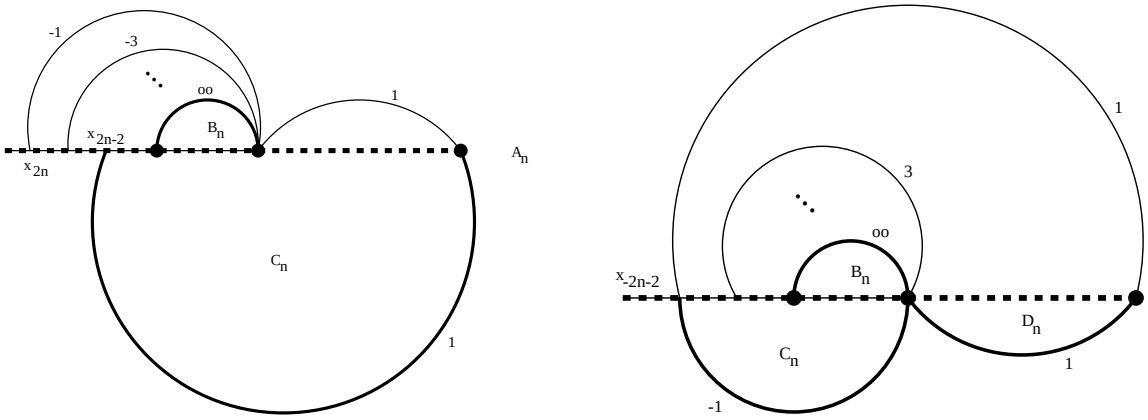

Fig. 16: Shown is a sketch, for $m > \frac{\Lambda_2}{2}$, of the relative positions of the decay curves of a generic dyon $(2n+1,1)_1$ with $n \geq 1$ in the left figure and $n \leq -2$ in the right figure. We have not shown the curves inside the $r = \infty$ curves. The thick curves are the relevant ones.

Now, for a generic dyon $(2n+1,1)_1$ with $n \geq 1$ one has the situation of the left Fig. 16. Of course, for $n = 1$, i.e. for the dyon $(3,1)_1$, the $r = 1$ curve for $\epsilon < 0$ starts at $x_0 \equiv \sigma_1$, but this makes not much difference. Decays are only possible on the $r = \infty$ curve and the $r = 1$ curve for $\epsilon < 0$. By the same arguments as above it is clear (for $n \geq 1$) that $(2n+1,1)_1$ cannot exist in regions B_n or C_n. The decays are $(2n+1,1)_1 \to (n+1) \times (1,1)_1 + (-n) \times (-1,1)_1$ on the $r = \infty$ curve which is $\mathcal{C}^\infty$ in the upper half plane, and $(2n+1,1)_1 \to 2 \times (1,0)_1 + (2n-1,1)_{-1}$ on the $r = 1$ curve which is $\mathcal{C}_{2n}^-$ in the lower half plane.

Next, for the dyons $(2n+1,1)_1$ with $n \leq -2$, we have the situation of the right Fig 16. The kinematically possible decays are: $(2n+1,1)_1 \to 2 \times (1,0)_1 + (2n-1,1)_{-1}$ on the $r_{\rm d} = 1$ curve for $\epsilon < 0$ ($\mathcal{C}_{2n}^-$), $(2n+1,1)_1 \to (-2) \times (1,0)_{-1} + (2n+3,1)_{-1}$ on the $r_{\rm d} = -1$ curve for $\epsilon < 0$ ($\mathcal{C}_{2n+2}^+$), and $(2n+1,1)_1 \to (-n) \times (-1,1)_1 + (n+1) \times (1,1)_1$ on the $r_{\rm d} = \infty$ curve for $\epsilon > 0$ ($\mathcal{C}^\infty$). By the $(M_{2\cdot3}^*)^{\pm1}$ and M_3^* arguments one sees that $(2n+1,1)_1$ with $n \leq -2$ cannot exist in regions B_n, C_n and D_n.

The dyons $(2n+1,1)_{-1}$ exist in the complex conjugate domains of where the $(-2n-1,1)_1$ exist. All this is shown in Fig. 13.

The quarks $(1,0)_{\pm 1}$

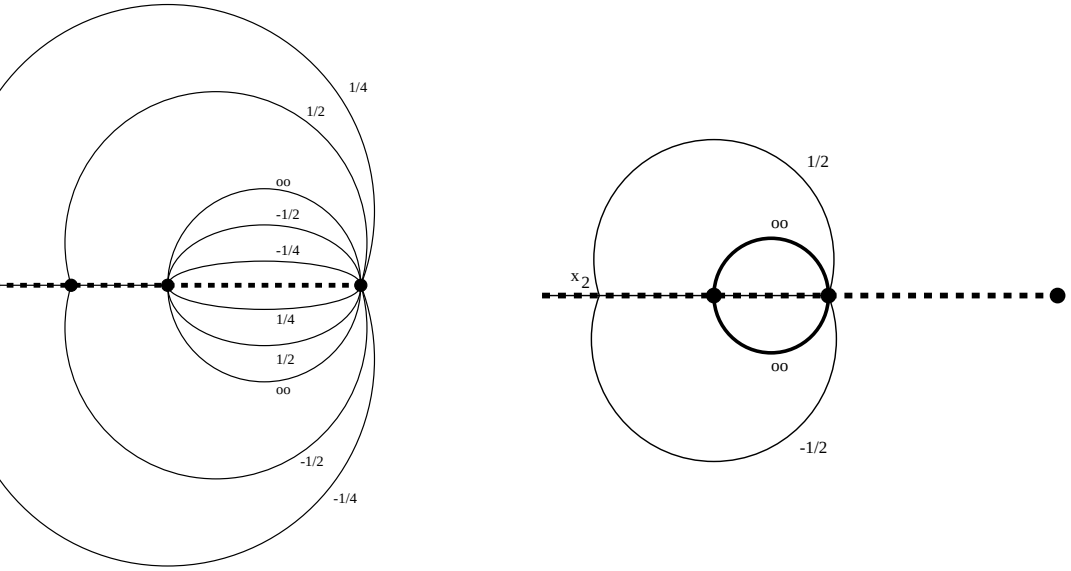

Fig. 17: Shown is a sketch, for $m > \frac{\Lambda_2}{2}$, of the relative positions of the decay curves of the quark $(1,0)_1$ (left) and of the quark $(1,0)_{-1}$ (right). For the latter, we have not shown the curves $r > 0$ inside the $r = \infty$ curve. The thick curves are the relevant ones.

First, the quark $(1,0)_1$ is massless at σ_3. All curves go through σ_3, see Fig. 17, and we conclude that this quark exists everywhere!

For the other quark $(1,0)_{-1}$, the curves are shown in the right Fig. 17. Decays are only possible on the $r = \infty$ curve ($\mathcal{C}_0^+$) where they are $(1,0)_{-1} \to (0,1)_0 + (-1) \times (-1,1)_1$ for $\epsilon > 0$ and $(1,0)_{-1} \to (-1) \times (0,1)_0 + (1,1)_{-1}$ for $\epsilon < 0$. The quark $(1,0)_{-1}$ cannot exist inside the $r = \infty$ curve since again this would imply the existence of a state $(M_{2\cdot 3}^*)^{\pm 1}(1,0)_{-1} = (0, \mp 1)_{-2}$ that does not exist.

The W-boson $(2,0)_0$

For the W-boson, there is no $r = \infty$ curve, and the $r = \pm 1$ curves exist only for $\epsilon = \pm 1$, where they actually are $\mathcal{C}^\infty$. By the $(M_{2\cdot 3}^*)^{\pm 1}$ argument, the W-boson cannot exist inside $\mathcal{C}^\infty$. The decays are $(2,0)_0 \to (1,1)_\epsilon + (-1) \times (-1,1)_\epsilon$.

5. Physical discussion : the $N = 2$ superconformal fixed points

In the light of our preceding results, we now discuss the physics of the superconformal points.

At a point u_* on the Coulomb branch where mutually non-local dyons become massless, the low energy theory is believed to be an interacting superconformal field theory [6]. In the theories we studied in this paper, such a point occurs when two singularities coincide [7]. Near u_* which always lies in a region where the low energy theory is strongly coupled (independently of the choice of variables), the masses of the particles becoming massless at u_* are much smaller than the masses of all the other particles (which are of order Λ) and set a new mass scale M. This implies that one can give an intrinsic meaning to the superconformal field theory (SCFT) independently of its embedding in the original non-abelian gauge theory, by letting $\Lambda \to \infty$. Actually, the *same* $N = 2$ SCFT can be embedded in different $N = 2$ non-abelian gauge theories. Argyres and Douglas were able to show, in a particular but generic case that corresponds in our language of Section 2.1 to a $k = 1$ SCFT, that the low energy coupling does not depend on the separation of scales Λ/M. This is a strong indication that the coupling does not run between the scales M and Λ, and thus very convincing evidence that the theory indeed has conformal invariance. One of the most striking properties of these SCFTs is that they do not contain any gauge boson that could contribute to the β function with a minus sign. We have seen this in great detail in Section 4 for the $k = 2$ superconformal point appearing in the $N_f = 2$ theory, since the only spin one particle at this point has quantum numbers $(2, 0)_0$ and a mass $\Lambda_2/\sqrt{2} \neq 0$. It is easy to realize that this is also the case at any superconformal point appearing in the $1 \leq N_f \leq 3$ theories. To explain that the β function can nevertheless be zero, Argyres and Douglas [6] suggested a simple ansatz which consists in computing the perturbative contribution of each hypermultiplet which occurs in the SCFT separately. This is done by using duality to go to a formulation of the theory where the given hypermultiplet is described locally, and then to apply the inverse duality transformation to the contribution to the beta function. The individual terms are then simply added to obtain the total β function:

$$\frac{\partial \tau}{\partial \log \mu} = -\frac{i}{2\pi} \sum \Big(n_m \tau - n_e \Big)^2 . \tag{5.1}$$

where each state $(n_e, n_m)_s$ in the sum should be counted with its correct multiplicity d. Of course, it is by no means obvious why this should give the correct answer.* In this equation, $\tau = \theta/\pi + 8i\pi/g^2$ is the (generalized) coupling of a theory containing the hypermultiplets (n_e, n_m) over which the sum is done. This is not the low energy coupling of the original gauge theory which, to avoid confusion, we will hereafter denote $\tau_{\text{eff}} = da_D/da$.

To discuss the validity of this ansatz (5.1) remark that it has three immediate and important consequences noted in [6]. The first one is that the θ angle does run, due to the contribution of magnetically charged states. This is quite surprising in a U(1) theory, and this effect

$\star$ An early and somewhat related discussion can be found in ref. 22.

may well remain qualitatively valid and have interesting consequences in non-supersymmetric theories as well, perhaps by shading a new light on the strong CP problem. However, we will have nothing new to say about this in the following. The second consequence of (5.1) is that we have an RG fixed point with a fixed point coupling τ_* satisfying

$$\sum \Big(n_m \tau_* - n_e \Big)^2 = 0. \tag{5.2}$$

The third consequence is that this fixed point is IR stable, the slope ω of the β function being positive, with (5.1) giving

$$\omega = \Re e \lim_{\tau \to \tau_*} \frac{1}{\tau - \tau_*} \frac{\partial(\tau - \tau_*)}{\partial \log \mu} = \frac{\sum n_m^2}{\pi} \, \Im m \, \tau_* > 0. \tag{5.3}$$

The positivity of ω is also required by unitarity [15]. In the following, we will argue that (5.2) is correct, but that (5.3) is wrong. This was already suspected in [6], since (5.3) gives irrational values for ω. We will see that the correct value for ω is indeed a rational number.

Before presenting our discussion, it is necessary to stress the following: although the effective coupling $\tau_{\rm eff}(u)$ and the running coupling $\tau_u(\mu)$ of the microscopic theory at fixed u and scale μ are different physical quantities, they are nevertheless related. The easiest way to understand this is to first choose u near a singular point u_0 where only locally related states become massless, a familiar case. At fixed u, the particle spectrum of the theory consists of the BPS states becoming massless at u_0 and having masses $M \sim t(u - u_0)$ where t is a constant, and of other states of mass $\sim \Lambda$ or higher. The dependence of M on u simply means that u is a good local coordinate near u_0, or, in terms more appropriate for the discussion to come, that u has dimension one. This is equivalent to the fact that the low energy theory is *free* massless super-QED. The effective coupling $\tau_{\rm eff}$ for a given u then corresponds to the microscopic running coupling $\tau_u(\mu)$ at a scale $\mu \sim M$ or lower. Between the scales M and Λ, $\tau_u(\mu)$ is given reliably, after a duality transformation which renders the theory weakly coupled in the IR, by a one loop calculation in ordinary $N = 2$ super-QED coupled only with the states of masses $\sim M$. One then identifies $\tau_{\rm eff}(u)$ with $\tau_u(\mu = M)$ to find the asymptotic behaviour of $\tau_{\rm eff}$ near the singularity [1,2]. Similarly, using the same argument backwards, and repeating this reasoning near a superconformal point u_* where $\tau_{\rm eff}$ is known via our explicit formulas (e.g. (2.27) for the $k = 2$ SCFT), one can deduce the form of $\tau_u(\mu)$. Hence the effective coupling at u_* must coincide with the fixed point coupling τ_*:

$$\tau_{\rm eff}(u_*) = \tau_* \ . \tag{5.4}$$

Furthermore, we will see below that $\tau_{\rm eff}$ has the following asymptotic behaviour,

$$\tau_{\rm eff}(u) = \tau_* + C(u - u_*)^\gamma + o\big((u - u_*)^\gamma\big). \tag{5.5}$$

Moreover, it follows from eq. (2.13) that at u the masses of the particles becoming massless at u_* are $M \sim t(u - u_*)^{1/\alpha}$, and that α is the anomalous dimension of u. We deduce that

$\tau - \tau_* \sim \mu^{\alpha\gamma}$ and thus that the slope ω of the β-function is given by

$$\omega = \alpha\gamma. \tag{5.6}$$

Let us first exploit the fact that $\tau_{\rm eff}(u_*) = \tau_*$ to discuss (5.2). Naively, at a superconformal point where two singularities coincide, one has precisely two massless states. For instance, at the $k = 3$ superconformal point of the $N_f = 3$ theory depicted in Fig. 2, one would expect to have the states $(1,1)_2$ and $(1,2)_3$. However, with these states, (5.2) does not give the correct answer for the fixed point coupling, which in this case is $\tau_* = e^{i\pi/3} = \tau_{\rm eff}(u_*)$. The solution to this puzzle is not to give up (5.2), but to realize that there are other states which become massless at the superconformal points. One way to find them is to look for massless states in the maximal set of BPS states of the $N_f = 3$ theory. This is correct because one can show, along the lines of Section 4, that all the states belonging to the maximal set must exist at the superconformal point. Thus we deduce that we have six massless states, three triplets $(1,1)_2$, $(0,1)_1$ and $(1,0)_1$, and three singlets $(1,2)_3$, $(-1,1)_0$ and $(2,1)_3$. With these states (5.2) gives the right answer. One interesting point to note is the following: the states being massless at the potentially coinciding singularities for small masses ($m < \Lambda_3/8$), i.e. $(1,1)_2$ and $(1,2)_3$, and the states becoming massless for large masses ($m > \Lambda_3/8$), i.e. $(-1,1)_0$ and $(1,0)_1$, are four *distinct* states and not simply analytic continuations of each other. The mechanism which allows to change the quantum numbers at the singularities in the asymptotically free theories, a phenomena which was known to occur since the work of Seiberg and Witten [1,2], is thus fully elucidated: at a point where two singularities collide, new states become massless "accidentally" and, when the singularities split again, these new states can take over the rôles of the original massless states which were responsible for the singularities before the collision.

Let us illustrate this mechanism in more detail in the case of the $N_f = 2$ theory studied in Section 4. Figure 18 represents an enlargement of Figs. 4 and 13 near the singularities. We explicitly indicate the existing states in the different regions surrounded by the curves of marginal stability. Since $a_D = a - \frac{m}{\sqrt{2}} = 0$ at the superconformal point, it is clear from Figure 18 that the states becoming massless at this point are the two singlets $(-1,1)_{-1}$ and $(1,1)_1$, and the two doublets $(0,1)_0$ and $(1,0)_1$. Equation (5.2) then gives the correct fixed point coupling, $\tau_* = i$. When $m < \Lambda_2/2$, the states responsible for the singularities are $(-1,1)_{-1}$ and $(0,1)_0$, and exist everywhere on the Coulomb branch. The states $(1,1)_1$ and $(1,0)_1$ are also very special, since they exist everywhere except inside the innermost curve $\mathcal{C}_0^-$. This is a nice test of the spectra derived in Section 4, since $(1,1)_1$ and $(1,0)_1$, being massless at the superconformal point, must exist everywhere except possibly inside curves of marginal stability shrinking to zero when such a point is approached. This is indeed what happens for the curve $\mathcal{C}_0^-$. When $m > \Lambda_2/2$, the rôles of the states $(-1,1)_{-1}$, $(0,1)_0$ and $(1,1)_1$, $(1,0)_1$ are exchanged but the picture still is perfectly coherent because $(-1,1)_{-1}$ and $(0,1)_0$ again exist everywhere outside $\mathcal{C}_0^-$.

Let us mention that at the $k = 1$ SCFT appearing in the $N_f = 1$ theory, we have three massless states which correspond exactly to the three states which were identified in [6] at the $\mathbf{Z}_3$ point of the SU(3) moduli space. This was expected since the two SCFTs are believed [7]

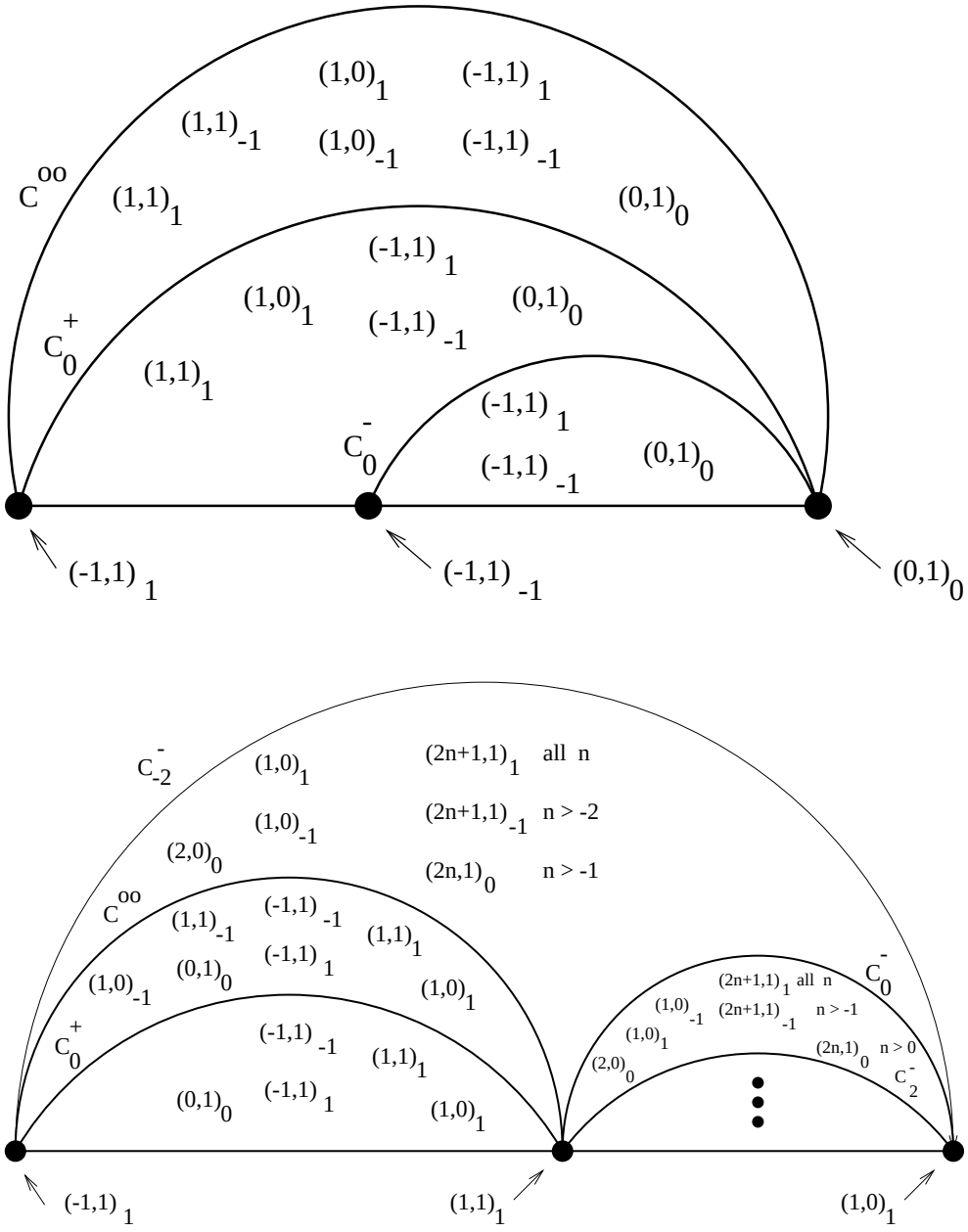

Fig. 18: The curves of marginal stability and stable BPS states in the upper half u-plane near the singularities in the $N_f = 2$ theory with $m_1 = m_2 = m$. The upper configuration corresponds to $m < \Lambda_2/2$ and the lower configuration to $m > \Lambda_2/2$.

to be the same. It would be interesting to check whether such a correspondence between states still holds for the $k = 2$ and $k = 3$ SCFT when these theories are embedded in the SU(4) or SO(8) pure gauge theories [16].

There is still one unsatisfying point in the above discussion. Though we saw that (5.2) gives the correct fixed point coupling, its application requires the knowledge of the set of all the massless states, which from the above discussion seems to depend crucially on the theory in which the SCFT is embedded. This is not natural since τ_* is, at least modulo a duality transformation, a characteristic of the SCFT. Actually, the massless spectra can be deduced from the local data only. Indeed, as the original massless states exist everywhere on the Coulomb branch and cannot decay, one can produce new massless states by encircling the superconformal singular point. The massless spectra must then be invariant under the monodromy $M_{\rm sc}$ at the superconformal point. This invariance only generates a finite number of new states because $M_{\rm sc}$ is of finite order. Using this invariance, one can deduce straightforwardly the massless BPS spectra uniquely from the quantum numbers of the colliding singularities. For instance, by applying (4.4) on the states $(-1,1)_{-1}$ and $(0,1)_0$, one generates exactly the two missing states $(1,1)_1$ and $(1,0)_1$.

It is very tempting to conjecture that the matrix $M_{\rm sc}$ always corresponds to an exact quantum duality symmetry of the SCFT. In addition to the invariance of the spectrum, this is supported by the (related) fact that the fixed point couplings satisfy $M_{\rm sc}\cdot\tau_*=\tau_*$ and by the fact that the symmetry $M_{\rm sc}$ can be realized as a global symmetry e.g. as the $\mathbf{Z}_3$ symmetry of the $k=1$ SCFT when embedded in the SU(3) pure gauge theory. Note that the surprising idea that global symmetries can be related to non-trivial duality transformations was first realized and used in [3] in the case of the $\mathbf{Z}_2$ symmetry acting on the moduli space of the SU(2) pure gauge theory. We find a very explicit realization of this fact with the superconformal points studied in this paper. Very recently, this idea has also been used very nicely to study S duality in some finite gauge theories [17]. We strongly feel that this is a very interesting point of view, since it relates a priori purely quantum symmetries to more conventional symmetries which have a classical origin.

Let us now turn to the computation of ω. We will also obtain α, recovering the results of [7]. To compute these two critical exponents, it is enough to find the asymptotic expansions of a_D and a near u_* up to the second order. An easy way to deduce the result is the following: diagonalizing the monodromy matrix $M_{\rm sc}$, its eigenvalues are $x_\pm=\exp(\pm\frac{i\pi}{6}(1+k))$, which shows that the leading power in the expansion, corresponding to $1/\alpha$, see (2.13), must be of the form

$$\frac{1}{\alpha}=\pm\frac{1+k}{12}+n\ ,\quad n\in\mathbf{Z}.$$

Imposing $\alpha\geq 1$ which is a necessary condition for a unitary SCFT [7], and $\alpha\leq 2$ which amounts to saying that the operator u is relevant, the only possibility is that α is related to the eigenvalue x_- with $n=1$,

$$\alpha=\frac{12}{11-k}. \tag{5.7}$$

The other eigenvalue x_+ is related to the subleading power $1/\beta>1/\alpha$ in the expansion by

$$\frac{1}{\beta}=+\frac{1+k}{12}+1=\frac{13+k}{12}. \tag{5.8}$$

The formulae (5.7) and (5.8) can be checked using the explicit solutions given in (2.27) for $N_f = 2$ or those in Appendix C for the other cases. By using

$$\begin{aligned} a_D(u) =& a_D(u_*) + c_D(u-u_*)^{1/\alpha} + c'_D(u-u_*)^{1/\beta} + o\big((u-u_*)^{1/\beta}\big) \\ a(u) =& a(u_*) + c(u-u_*)^{1/\alpha} + c'(u-u_*)^{1/\beta} + o\big((u-u_*)^{1/\beta}\big) \end{aligned}$$

and the relation $\tau_{\text{eff}} = da_D/da$, we deduce that the exponent γ of (5.5) is given by $\gamma = 1/\beta - 1/\alpha$, and thus $\omega = \alpha\gamma$ is

$$\omega = \frac{2+2k}{11-k}. \tag{5.9}$$

This is a rational number which differs from (5.3). This implies that despite its appealing features, the Argyres-Douglas ansatz (5.1) cannot be exact. The problem of finding the general form of the β function for these non-local field theories thus remains open. Maybe one can guess the result by using the exact solutions for τ_{eff} presented in this paper around the superconformal points and use the arguments above to relate τ_{eff} and τ.

A simple inspection of the formulae (5.7) and (5.9) reveals that the two exponents α and ω are related by

$$\omega = 2(\alpha - 1). \tag{5.10}$$

Such a "scaling" relation is possible because, due to $N = 2$ supersymmetry, the only free parameter is k and thus one expects only one independent critical exponent. It is actually possible to understand (5.10) on general grounds, following the line of reasoning of [7]: if we denote by U the U(1) $N = 2$ vector superfield contained in the low energy effective action at a generic point on the Coulomb branch, a deviation of the coupling constant from its fixed point value corresponds to the irrelevant (since the fixed point is IR stable) operator

$$\delta L_{\text{eff}} = \Lambda^{-\omega} \int d^4\theta \, U^2,$$

where the fermionic integration is performed over half of $N = 2$ superspace. As the dimension of L_{eff} must be 4 since the action is dimensionless, and the dimension of $d^4\theta$ is two, we must have $-\omega + d_{U^2} = 2$ where d_{U^2} is the dimension of the operator U^2. Because of *super*conformal invariance, we must have $d_{U^2} = 2d_U = 2\alpha$ because these scaling dimensions are directly proportional to the R charges of U and U^2 under the exact *quantum* $\text{U}(1)_R$ symmetry of the superconformal algebra. We thus recover the relation (5.10). Conversely, one can consider (5.10) as a non-trivial test that the theory has indeed $N = 2$ superconformal invariance.

APPENDIX A

For reference, in this appendix we briefly discuss the positions of the singularities and their flows for the massive $N_f = 1, 2, 3$ theories. For simplicity, all non-zero bare masses are taken to be equal.

$N_f = 3$ with $m_1 = m_2 = m_3 \equiv m$

For $m \neq 0$ the flavour symmetry is SU(3), while for $m = 0$ it is spin(6) $\simeq$ SU(4). For the present case, the discriminant of the cubic polynomial (2.1), (2.2) in x is

$$\begin{aligned}\Delta = \frac{\Lambda_3^2}{16}\left(-u + m^2 + \frac{\Lambda_3}{8}m\right)^3 \\ \times\left[u^2 + \left(\frac{3}{8}\Lambda_3 m - \frac{\Lambda_3^2}{256}\right)u - \Lambda_3 m^3 - \frac{3}{256}\Lambda_3^2 m^2 - \frac{3}{2048}\Lambda_3^3 m\right]\end{aligned} \tag{A.1}$$

showing that there is a triple singularity σ_t, transforming as the **3** of SU(3), and two singlet singularities $\sigma_\pm$ at

$$\sigma_t = m^2 + \frac{\Lambda_3}{8}m \quad , \quad \sigma_\pm = -\frac{3}{16}\Lambda_3 m + \frac{\Lambda_3^2}{512} \pm \Lambda_3^{1/2}\left(m + \frac{\Lambda_3}{64}\right)^{3/2} . \tag{A.2}$$

For small m one has $\sigma_+ \simeq \frac{\Lambda_3^2}{256}$ and $\sigma_- \simeq -\frac{3}{8}\Lambda_3 m$, and at $m = 0$, σ_- and σ_t coincide and one has a quadruple singularity at $u = 0$ corresponding to a massless dyon of magnetic charge one which transforms as the **4** of SU(4). The singularity at σ_+ is due to a massless dyon of magnetic charge two [2] (see Fig. 2). As m is increased, the singlet σ_- moves to the left and the triplet moves to the right. The singularities σ_t and σ_+ meet at

$$m = \frac{\Lambda_3}{8} \quad , \quad \sigma_t = \sigma_+ = \frac{\Lambda_3^2}{32} = 2m^2 . \tag{A.3}$$

which is the superconformal point. As m is increased further, as discussed in Section 2, the quantum numbers at the singularities are changed and now are $(1,1)_0$ and $(-1,1)_0$ at σ_- and σ_+ and a quark triplet at σ_t. The latter disappears to infinity as $m \to \infty$, $\Lambda_3 \to 0$, $m^3\Lambda_3 = \Lambda_0^4$ fixed, while $\sigma_\pm \to \pm\Lambda_0^2$, and indeed, (after rotating the quark cut to the right and shifting $a_D \to a_D + a$) we are left with the pure gauge theory $N_f = 0$.

$N_f = 3$ with $m_1 = m_2 = 0$ and $m_3 \equiv m$

For this case, the roots of the cubic are at $x = u$ and $x = \frac{\Lambda_3^2}{128} \pm \left[\frac{\Lambda_3^2}{256}\left(\frac{\Lambda_3^2}{64} - 4u + 4m^2\right)\right]^{1/2}$. Thus there is a singlet singularity at σ_s and two doublet singularities at $\sigma_d^\pm$:

$$\sigma_s = m^2 + \frac{\Lambda_3^2}{256} \quad , \quad \sigma_d^\pm = \pm\frac{\Lambda_3}{8}m . \tag{A.4}$$

As m is increased from 0, the quadruple singularity at the origin splits into two doublets of massless monopoles (having different values of s) while the singlet at σ_s starts to move to the

right. But σ_d^+ moves faster to the right and meets σ_s at the superconformal point

$$m = \frac{\Lambda_3}{16} \quad , \quad \sigma_d^+ = \sigma_s = \frac{\Lambda_3^2}{128} = 2m^2 \ . \tag{A.5}$$

As m is increased beyond $\frac{\Lambda_3}{16}$, σ_s remains larger than σ_d^+ and the singularity at σ_s is now due to a (singlet) massless quark, while the other two doublet states at σ_d^+ and σ_d^- now are a magnetic monopole and the dyon with $n_e = \mp 1$ both having vanishing s. As $m \to \infty$, $m\Lambda_3 = \Lambda_2^2$ fixed, the massless quark at σ_s dissappears to infinity, while $\sigma_d^\pm \to \pm\frac{\Lambda_2^2}{8}$, and one is left with the massless $N_f = 2$ theory.

$N_f = 2$ with $m_1 = m_2 \equiv m$

This case was discussed in great detail in the main body of this paper, see Section 2.

$N_f = 2$ with $m_1 = 0$ and $m_2 \equiv m$

In this case the flavour symmetry is only $\mathrm{U}(1) \times \mathrm{U}(1)$ for $m \neq 0$. The discriminant of the cubic is

$$\Delta = \frac{\Lambda_2^4}{16}\left[u^4 - m^2u^3 - \frac{\Lambda_2^4}{32}u^2 + \frac{9}{64}\Lambda_2^4 m^2 u + \frac{\Lambda_2^8}{4096} - \frac{27}{256}\Lambda_2^4 m^4\right] \ . \tag{A.6}$$

For $m = 0$ we have two doublets of massless monopoles and dyons in one and the other spinor representation of spin(4) at $u = \pm\frac{\Lambda_2^2}{8}$. For small non-zero mass m each of these doublets splits into two singlets at

$$\sigma_-^\pm = -\frac{\Lambda_2^2}{8} \pm \frac{\Lambda_2}{2}m + \mathcal{O}(m^2) \quad , \quad \sigma_+^\pm = \frac{\Lambda_2^2}{8} \pm i\frac{\Lambda_2}{2}m + \mathcal{O}(m^2) \ . \tag{A.7}$$

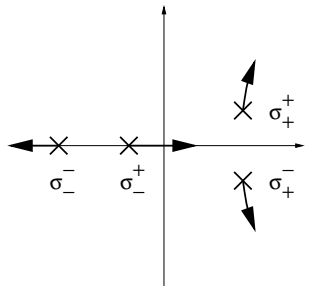

Fig. 19: The flow of the singularities on the complex u-plane for $N_f = 2$, $m_1 = 0$ and small $m_2 = m$

Two singularities move off the real axis into the complex plane, see Fig. 19. As m is increased σ_-^+ moves to the right on the real axis, much faster than the other singularities. It passes between σ_+^+ and $\sigma_+^- = (\sigma_+^+)^*$. As $m \to \infty$, $\sigma_-^+ \to \infty$, while σ_-^- and $\sigma_+^\pm$ arrange

themselves on a circle at the roots of $u^3 + \frac{27}{256}\Lambda_2^4 m^2 = 0$. Since $m\Lambda_2^2 = \Lambda_1^3$ these are precisely the singularities of the massless $N_f = 1$ theory. In the present case, while flowing from $m = 0$ to $m = \infty$, we never encounter a superconformal point where singularities coincide. Nevertheless, the quantum numbers of the massless states change by the monodromy matrix of another singularity as explained in Section 2.

The $N_f = 1$ theory

The discriminant is

$$\Delta = \frac{\Lambda_1^6}{16}\left[-u^3 + m^2u^2 + \frac{9}{8}\Lambda_1^3 mu - \Lambda_1^3 m^3 - \frac{27}{256}\Lambda_1^6\right] . \tag{A.8}$$

The positions of the singularities are given by the three roots of this cubic polynomial in u:

$$\sigma_0 = \alpha_+ + \alpha_- + \frac{m^2}{3} \quad , \quad \sigma_\pm = \mathrm{e}^{\pm 2i\pi/3}\alpha_+ + \mathrm{e}^{\mp 2i\pi/3}\alpha_- + \frac{m^2}{3} . \tag{A.9}$$

The massless states are all singlets. The $\alpha_\pm$ are given by

$$\alpha_\pm = \frac{1}{3}\left\{ m^6 - \frac{135}{16}\Lambda_1^3 m^3 - \frac{729}{512}\Lambda_1^6 \pm \left[27\Lambda_1^3\left(\frac{27}{64}\Lambda_1^3 - m^3\right)^3\right]^{1/2}\right\}^{1/3} . \tag{A.10}$$

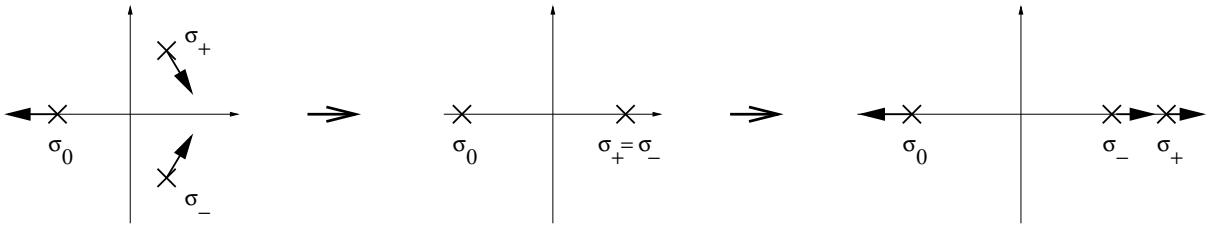

Fig. 20: The flow of the singularities for $N_f = 1$. The left figure shows the positions of the singularities for small mass m, the middle figure shows them at the superconformal point where σ_+ and σ_- coincide, while the right figure shows them for large m.

While the choice of phase of the square root does not really matter since one can always exchange the rôles of α_+ and α_-, the phase of the cubic root has to be determined carefully, so that the three singularities σ are either all real or one real and the other two complex conjugate, and such that the singularities vary continuously as m is varied from 0 to ∞. In particular, for $0 < m^3 < \frac{27}{64}\Lambda_1^3$ the curly bracket in (A.10) is real and negative, and we choose $\alpha_\pm = -\frac{1}{3}|\{\ldots\}|^{1/3}$. This ensures that σ_0 is real and negative, while σ_+ and σ_- are complex conjugate. For $m = 0$ one simply has $\sigma_0 = -u_0$, $\sigma_\pm = \mathrm{e}^{\pm i\pi/3}u_0$ with $u_0 = 3\Lambda_1^2/(4 \cdot 2^{2/3})$. As

m is increased, σ_0 moves to the left and $\sigma_\pm$ approach the real axis, see Fig. 20. For small m one has

$$\sigma_0 \simeq -u_0(1+2\mu) \quad , \quad \sigma_\pm \simeq u_0\left(\mathrm{e}^{\pm i\pi/3} + 2\mu \mathrm{e}^{\mp i\pi/3}\right) \tag{A.11}$$

where $\mu = 2\cdot 2^{1/3} m/(3\Lambda_1) \ll 1$. When the square root in (A.10) vanishes, $\alpha_+ = \alpha_-$, so that σ_+ and σ_- meet on the real axis. This is a superconformal point:

$$m = \frac{3\Lambda_1}{4} \quad , \quad \sigma_+ = \sigma_- = \frac{4}{3}m^2 = \frac{3\Lambda_1^2}{4} \ . \tag{A.12}$$

As m is increased further, the curly bracket in (A.10) is now complex. We choose $[\ldots]^{1/2} = -i|[\ldots]|^{1/2}$. (The opposite choice only exchanges σ_+ and σ_-.) The phase of the cubic root is chosen so that $\alpha_+ = \alpha_-^*$ with $\frac{2\pi}{3} < \arg\alpha_+ < \pi$ and $-\pi < \arg\alpha_- < -\frac{2\pi}{3}$. With this choice, the singularities will flow continuously: σ_0 keeps moving to the left, while $\sigma_\pm$, now both real, move to the right, but σ_+ moves faster, see Fig. 20. As $m \to \infty$, one has

$$\sigma_0 \simeq -(\Lambda_1^3 m)^{1/2} \quad , \quad \sigma_- \simeq (\Lambda_1^3 m)^{1/2} \quad , \quad \sigma_+ \simeq m^2 \tag{A.13}$$

up to terms $\mathcal{O}(\Lambda_1^3/m)$. Since $\Lambda_1^3 m = \Lambda_2^4$, σ_0 and σ_- flow to the singularities of the pure gauge theory, while σ_+ disappears to infinity.

APPENDIX B

In this appendix we will show how to express the integrals $I_i^{(j)}$ in terms of the standard elliptic integrals $K(k)$, $E(k)$, $\Pi_1(\nu,k)$, and also give their expressions in terms of the Weierstraß $\wp$ function, as well as give certain relations between elliptic integrals. Basic references are [14, 19, 20]. Our conventions are those of [14]. Unless otherwise stated, we will assume that the roots e_i of the cubic $\eta^2 = 4\xi^3 - g_2\xi - g_3$ are all different. They obey $\sum_i e_i = 0$, and $\eta^2 = 4\prod_i(\xi - e_i)$.

The K, E and Π_1 only depend on the square of k which was defined in terms of the e_i as $k^2 = \frac{e_2-e_3}{e_1-e_3}$. We use the notation* of [14]:

$$\begin{aligned} K(k) &= \int_0^1 \frac{\mathrm{d}x}{\left[(1-x^2)(1-k^2x^2)\right]^{1/2}} \\ E(k) &= \int_0^1 \mathrm{d}x \left(\frac{1-k^2x^2}{1-x^2}\right)^{1/2} \\ \Pi_1(\nu,k) &= \int_0^1 \frac{\mathrm{d}x}{\left[(1-x^2)(1-k^2x^2)\right]^{1/2}(1+\nu x^2)} \ . \end{aligned} \tag{B.1}$$

$\star$ Note that in Mathematica which we used extensively for the numerical determination of the curves of marginal stability, one denotes $K(k) =$ `EllipticK`$[k^2]$, $E(k) =$ `EllipticE`$[k^2]$ and $\Pi_1(\nu,k) =$ `EllipticPi`$[-\nu, k^2]$.

We will now show that the integrals over the cycle γ_1 are

$$\begin{aligned} I_1^{(1)} &= 2\int_{e_3}^{e_2} \frac{\mathrm{d}\xi}{\eta} = \frac{2}{(e_1-e_3)^{1/2}}\, K(k) \\ I_2^{(1)} &= 2\int_{e_3}^{e_2} \frac{\xi \mathrm{d}\xi}{\eta} = \frac{2}{(e_1-e_3)^{1/2}}\, \left[e_1 K(k) + (e_3-e_1)E(k)\right] \\ I_3^{(1)} &= 2\int_{e_3}^{e_2} \frac{\mathrm{d}\xi}{\eta(\xi-c)} = \frac{2}{(e_1-e_3)^{3/2}} \left[\frac{1}{1-\tilde{c}+k'}\, K(k) \right. \\ &\qquad \left. + \frac{4k'}{1+k'}\, \frac{1}{(1-\tilde{c})^2-k'^2}\, \Pi_1\left(\nu(c), \frac{1-k'}{1+k'}\right)\right] \end{aligned} \tag{B.2}$$

where

$$k'^2 = 1-k^2 \quad , \quad \tilde{c} = \frac{c-e_3}{e_1-e_3} \quad , \quad \nu(c) = -\left(\frac{1-\tilde{c}+k'}{1-\tilde{c}-k'}\right)^2 \left(\frac{1-k'}{1+k'}\right)^2 . \tag{B.3}$$

The corresponding integrals $I_i^{(2)}$ over the cycles γ_2 are obtained from equations (B.2) and (B.3) by exchanging everywhere in these equations the roots e_1 and e_3. In particular, this exchanges k and k', and results in the exchange of $\tilde{c}$ and $1-\tilde{c}$, so that $\nu(c)$ gets replaced by $-\left(\frac{\tilde{c}+k}{\tilde{c}-k}\right)^2 \left(\frac{1-k}{1+k}\right)^2$.

To convert the I_j into the K, E, Π_1 one needs to transform the cubic curve into a quartic curve. Let's demonstrate this for $I_1^{(1)}$:

$$I_1^{(1)} = 2\int_{e_3}^{e_2} \frac{\mathrm{d}\xi}{\eta} = \int_{e_3}^{e_2} \frac{\mathrm{d}\xi}{[(\xi-e_1)(\xi-e_2)(\xi-e_3)]^{1/2}} = \frac{1}{(e_1-e_3)^{1/2}} \int_0^{k^2} \frac{\mathrm{d}\tilde{\xi}}{[(\tilde{\xi}-1)(\tilde{\xi}-k^2)\tilde{\xi}]^{1/2}} \tag{B.4}$$

where we changed variables , $\tilde{\xi} = (\xi-e_3)/(e_1-e_3)$, and introduced k^2 as above. The transformation to a quartic curve is achieved by the further change of variables

$$\tilde{\xi} = 1+k' + \frac{1}{\zeta - \frac{1}{2k'}} \tag{B.5}$$

where the complementary modulus k' is given by (B.3). (The choice of sign for k' does not matter.) A final rescaling $x = 2k'\,\frac{1+k'}{1-k'}\,\zeta$ yields

$$I_1^{(1)} = \frac{1}{(e_1-e_3)^{1/2}}\, \frac{2}{1+k'} \int_{-1}^{1} \frac{\mathrm{d}x}{\left[\left(1-\left(\frac{1-k'}{1+k'}\right)^2 x^2\right)(1-x^2)\right]^{1/2}} = \frac{2}{(e_1-e_3)^{1/2}}\, \frac{2}{1+k'}\, K\left(\frac{1-k'}{1+k'}\right) . \tag{B.6}$$

Using one of the standard relations between elliptic integrals with different moduli [14]

$$\frac{2}{1+k'}\,K\left(\frac{1-k'}{1+k'}\right) = K(k) \quad , \quad (1+k')\,E\left(\frac{1-k'}{1+k'}\right) = E(k) + k'K(k)\ , \tag{B.7}$$

one obtains the first equation (B.2).[⋆]

Going through exactly the same steps for the integral $I_2^{(1)}$ leads to

$$\begin{aligned} I_2^{(1)} &= \frac{1}{(e_1-e_3)^{1/2}}\,\frac{2}{1+k'}\int_{-1}^{1}\mathrm{d}x\,\frac{(e_1-e_3)\left[1+k'-2k'\left(1-\left(\frac{1-k'}{1+k'}\right)^2x^2\right)^{-1}\right]+e_3}{\left[\left(1-\left(\frac{1-k'}{1+k'}\right)^2x^2\right)(1-x^2)\right]^{1/2}} \\ &= \frac{2}{(e_1-e_3)^{1/2}}\,\frac{2}{1+k'}\Bigg[\left((e_1-e_3)(1+k')+e_3\right)K\left(\frac{1-k'}{1+k'}\right) \\ &\qquad\qquad -2k'(e_1-e_3)\,\Pi_1\left(-\left(\frac{1-k'}{1+k'}\right)^2,\frac{1-k'}{1+k'}\right)\Bigg]\ . \end{aligned} \tag{B.8}$$

Using the relation $(1-\bar{k}^2)\Pi_1(-\bar{k}^2,\bar{k}) = E(\bar{k})$ with $\bar{k} = (1-k')/(1+k')$, as well as the relations (B.7), one arrives at the second equation (B.2).

Finally for $I_3^{(1)}(c)$, going through the same steps leads to

$$\begin{aligned} I_3^{(1)}(c) = \frac{1}{(e_1-e_3)^{3/2}}\,\frac{2}{1+k'}\int_{-1}^{1}&\frac{\mathrm{d}x}{\left[\left(1-\left(\frac{1-k'}{1+k'}\right)^2x^2\right)(1-x^2)\right]^{1/2}} \\ &\times\frac{1}{1+k'-\tilde{c}}\left[1-\frac{2k'}{1+k'-\tilde{c}}\,\frac{1}{\frac{1-k'}{1+k'}x-\frac{1-k'-\tilde{c}}{1+k'-\tilde{c}}}\right] \end{aligned} \tag{B.9}$$

where $\tilde{c} = (c-e_3)/(e_1-e_3)$. The last term in this expression is of the type $\frac{1}{ax-b} = \frac{ax+b}{a^2x^2-b^2}$ and can be replaced by $\frac{b}{a^2x^2-b^2}$. It is then clear, using again (B.7) that one gets the third relation (B.2).

The integrals $I_3^{(j)}(c)$ can be simplified if c is one of the roots e_i. We will always consider $I_3^{(1)}(c)$. Everything can be translated for $I_3^{(2)}(c)$ if we permute everywhere k and k' as well as

⋆ Note that it is quite non-trivial to keep track of the correct overall sign. For example, to get the last equality of eq. (B.6) one needs to define carefully where the cuts of the differents square roots lie. For real masses m_i and real Λ, all one can get is a sign ambiguity that may depend on $\mathrm{sign}(\Im m\, u)$. This ambiguity is the same for all three integrals I_1, I_2 and I_3, so that it is most easily fixed by comparing the resulting a and a_D with the required asymptotics (2.25).

e_3 and e_1. Let first $c = e_1$. Then $\tilde{c} = 1$ and $\nu(c) = -\left(\frac{1-k'}{1+k'}\right)^2 \equiv -\tilde{k}^2$ (see (B.3)). One has [14]

$$\Pi_1(-\tilde{k}^2, \tilde{k}) = \frac{1}{1-\tilde{k}^2} E(\tilde{k}) = \frac{1+k'}{4k'} \left(E(k) + k'K(k)\right) \ . \tag{B.10}$$

Hence

$$I_3^{(1)}(e_1) = \frac{2}{(e_1-e_3)^{3/2}} \frac{E(k)}{k^2-1} \ . \tag{B.11}$$

This can also be directly obtained since $I_3^{(1)}(e_1) = 2\frac{\mathrm{d}}{\mathrm{d}e_1} I_1^{(1)}$. Using $k^2 \frac{\mathrm{d}}{\mathrm{d}k^2} K(k) = -\frac{1}{2}K(k) + \frac{1}{2}\frac{E(k)}{1-k^2}$ this gives again (B.11). Obviously, this constitutes a consistency check for the third equation (B.2). Let now $c = e_2$. Then $\tilde{c} = k^2$ and $\nu(c) = -1$. Π_1 is singular for $\nu = -1$, but $I_3^{(1)}(e_2)$ can be obtained in exactly the same way since $I_3^{(1)}(e_2) = 2\frac{\mathrm{d}}{\mathrm{d}e_2} I_1^{(1)}$ provided we keep the integration cycle γ_1 fixed and away from e_2 (and e_3). We then immediately get

$$I_3^{(1)}(e_2) = \frac{2}{(e_1-e_3)^{3/2}} \frac{1}{k^2} \left(\frac{E(k)}{1-k^2} - K(k)\right) \ . \tag{B.12}$$

Finally, if $c = e_3$, one has $\tilde{c} = 0$ and also $\nu(c) = -1$, and again Π_1 is singular, but we can still use $I_3^{(1)}(e_3) = 2\frac{\mathrm{d}}{\mathrm{d}e_3} I_1^{(1)}$ which readily gives

$$I_3^{(1)}(e_3) = \frac{2}{(e_1-e_3)^{3/2}} \frac{1}{k^2} \left(K(k) - E(k)\right) \ . \tag{B.13}$$

Of course, using the first two equations (B.2), one can reexpress $K(k)$ and $E(k)$ in terms of $I_1^{(1)}$ and $I_2^{(1)}$ and hence we have shown how to express $I_3^{(1)}(e_j)$ in terms of $I_1^{(1)}$ and $I_2^{(1)}$.

We also need to Taylor expand $I_3^{(j)}(c + \delta c)$, hence we want to compute the derivative $\frac{\mathrm{d}}{\mathrm{d}c} I_3^{(j)}(c)$. For any cycle γ_j we have

$$\frac{\mathrm{d}}{\mathrm{d}c} I_3^{(j)}(c) = \oint\limits_{\gamma_j} \frac{\mathrm{d}\xi}{\eta(\xi-c)^2} \ . \tag{B.14}$$

Now observe that

$$0 = \oint \mathrm{d}\xi \, \frac{\mathrm{d}}{\mathrm{d}\xi} \frac{\eta}{\xi - c} = \oint \mathrm{d}\xi \, \frac{12\xi^2 - g_2}{2\eta(\xi-c)} - \oint \mathrm{d}\xi \, \frac{\eta^2}{\eta(\xi-c)^2} \ . \tag{B.15}$$

This is a sum of integrals containing I_1, I_2 and I_3, as well as the integral (B.14). Solving for the latter gives

$$(4c^3 - cg_2 - g_3) \oint \frac{\mathrm{d}\xi}{\eta(\xi-c)^2} = -2c\, I_1 + 2\, I_2 - \frac{1}{2}(12c^2 - g_2)\, I_3(c) \ . \tag{B.16}$$

Inserting now the appropriate values of g_2 and g_3 for the $N_f = 1$ curve and taking $c = -u/3$

yields the desired relation for the derivative $I_3'(c) \equiv \frac{\mathrm{d}}{\mathrm{d}c} I_3(c)$:

$$-\frac{\Lambda_1^6}{32} I_3'\left(-\frac{u}{3}\right) = \frac{u}{3} I_1 + I_2 - \frac{m\Lambda_1^3}{4} I_3\left(-\frac{u}{3}\right) \ . \tag{B.17}$$

A word of caution is in order: in eq. (B.2) we have replaced the integrals over the cycle γ_1 by twice the integrals from e_3 to e_2. Depending on the detailed form of the cycle, these two definitions may differ for I_3, which has a pole at $\xi = c$, by terms $2\pi i \,\mathrm{res}\frac{\mathrm{d}\xi}{\eta}$. So we allow the freedom to add such terms "by hand", this being equivalent to changing the definition of the cycle γ_1 with respect to the position of the pole. A related point is that for $c = e_2$ or $c = e_3$, one has $\nu(c) = -1$ and $\Pi_1(-1, \tilde{k})$ diverges. Nevertheless, we can remove the divergence by an appropriate choice of integration contour.† With this choice $\Pi_1(-1, \tilde{k})$ should be understood as $K(\tilde{k}) - E(\tilde{k})/(1 - \tilde{k}^2)$. Then, eqs. (B.12) and (B.13) also follow in a straightforward manner, using (B.7), from the third equation (B.2). Similar remarks apply to the integrals $I_i^{(2)}$ over the cycles γ_2.

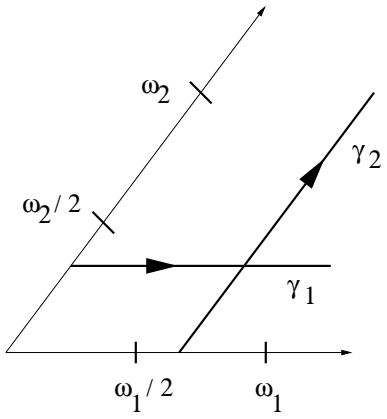

Fig. 21: The elliptic curve in the z-plane where it is simply a parallelogram with sides ω_1 and ω_2. The cycles γ_1 and γ_2 are straight lines parallel to the sides of the parallelogram.

To gain a somewhat better control over the integration cycles γ_1 and γ_2, in particular with respect to the positions of the poles, it is sometimes advantageous to introduce the uniformizing variable z via the doubly periodic Weierstraß $\wp$ function [19] as $\xi = \wp(z)$, $\eta = \wp'(z)$. Then the integrals $I_1^{(i)}$ are simply

$$I_1^{(i)} = \oint\limits_{\gamma_i} \frac{\mathrm{d}\xi}{\eta} = \int\limits_{\gamma_i} \frac{\wp'(z)\mathrm{d}z}{\wp'(z)} = \int\limits_0^{\omega_i} \mathrm{d}z = \omega_i \tag{B.18}$$

where ω_1 and ω_2 are the two periods of $\wp$ and are such that $e_1 = \wp\left(\frac{\omega_1}{2}\right)$, $e_2 = \wp\left(\frac{\omega_1+\omega_2}{2}\right)$,

† This is so because $\nu \to 1$ typically occurs under the RG flow as some bare mass $m_j \to \infty$ and the divergent part of Π_1 precisely is some integer multiple of $\frac{m_j}{2\sqrt{2}}$.

$e_3 = \wp\left(\frac{\omega_2}{2}\right)$. The cycle γ_1 is mapped in the z-plane to a straight line from 0 to ω_1 (or any shifted copy of it) while γ_2 is mapped to the straight line from 0 to ω_2, see Fig. 21.

Obviously one has $\tau = \frac{\omega_2}{\omega_1}$. Given the e_1, e_2, e_3, one can obtain ω_1 and ω_2, hence $I_1^{(1)}$ and $I_1^{(2)}$ using the inverse of the $\wp$ function. The latter is conveniently expressed through the inverse of the Jacobi elliptic function sn:

$$z_\xi \equiv \wp^{-1}(\xi) = \frac{1}{(e_1-e_3)^{1/2}}\ \mathrm{sn}^{-1}\left[\left(\frac{e_1-e_3}{\xi-e_3}\right)^{1/2}, k\right] \ . \tag{B.19}$$

For a numerical computation of the $\omega_i = I_1^{(i)}$, eq. (B.2) is of course simplest. Next one has (do not confuse the η_i with η)

$$I_2^{(i)} = \oint\limits_{\gamma_i} \frac{\xi \mathrm{d}\xi}{\eta} = -2\eta_i \tag{B.20}$$

where again numerical computation of the η_i is easiest done via (B.2). Finally, one has

$$I_3^{(i)} = \oint\limits_{\gamma_i} \frac{\mathrm{d}\xi}{\eta(\xi-c)} = \frac{1}{\wp'(z_c)}\left[2\omega_i\zeta(z_c) - 4\eta_i z_c\right] \tag{B.21}$$

where z_c is given by (B.19) with $\xi = c$, and

$$\zeta(z) = \frac{2\eta_1}{\omega_1}z + \frac{\pi}{\omega_1}\frac{\theta_1'}{\theta_1}\left(\frac{\pi z}{\omega_1}\Big|\tau\right) \ . \tag{B.22}$$

APPENDIX C

In this appendix we give the differentials λ for the different massive theories as well as the decomposition of the period integrals in terms of the three basic elliptic integrals I_1, I_2 and I_3. We also check some RG flows at the level of these integrals.

One flavour: $N_f = 1$

A one-form λ satisfying (2.4) obviously is

$$\lambda = -\frac{\sqrt{2}}{4\pi}\frac{y\,\mathrm{d}x}{x^2} = \frac{\sqrt{2}}{4\pi}\left[\mathrm{d}x\frac{\mathrm{d}}{\mathrm{d}x}\left(\frac{x}{y}\right) - \left(3x - 2u + \frac{\Lambda_1^3}{4}\frac{m}{x}\right)\frac{\mathrm{d}x}{2y}\right] \ . \tag{C.1}$$

The first term in the bracket is an exact form and vanishes upon integration over a cycle. Converting to Weierstraß normal form (2.21) by $\eta = 2y,\ \xi = x - \frac{u}{3}$ we get

$$\int \lambda = \frac{\sqrt{2}}{4\pi}\left[u\, I_1 - 3\, I_2 - \frac{\Lambda_1^3}{4} m\, I_3\left(-\frac{u}{3}\right)\right] \ . \tag{C.2}$$

We see from (C.1) that λ has poles at $(x = 0, y = \mp i\Lambda_1^3/8)$ with residues $\pm\frac{1}{2\pi i}\frac{m}{\sqrt{2}}$ in agreement with eq. (2.10).

Two flavours: $N_f = 2$

We have [2]

$$\begin{aligned}\lambda &= -\frac{\sqrt{2}}{4\pi}\frac{y\,\mathrm{d}x}{x^2-\frac{\Lambda_2^4}{64}} = -\frac{\sqrt{2}}{4\pi}\frac{\mathrm{d}x}{y}\frac{4y^2}{\Lambda_2^2}\left(\frac{1}{x-\frac{\Lambda_2^2}{8}}-\frac{1}{x+\frac{\Lambda_2^2}{8}}\right)\\ &= -\frac{\sqrt{2}}{4\pi}\frac{\mathrm{d}x}{y}\left[x-u-\frac{\Lambda_2^2}{16}\frac{(m_1-m_2)^2}{x-\frac{\Lambda_2^2}{8}}+\frac{\Lambda_2^2}{16}\frac{(m_1+m_2)^2}{x+\frac{\Lambda_2^2}{8}}\right]\ .\end{aligned} \tag{C.3}$$

Converting to Weierstraß normal form of the cubic, again by $\eta = 2y,\ \xi = x - \frac{u}{3}$ we arrive at

$$\int\lambda = \frac{\sqrt{2}}{4\pi}\left[\frac{4}{3}u\,I_1 - 2\,I_2 + \frac{\Lambda_2^2}{8}(m_1-m_2)^2\,I_3\left(\frac{\Lambda_2^2}{8}-\frac{u}{3}\right) - \frac{\Lambda_2^2}{8}(m_1+m_2)^2\,I_3\left(-\frac{\Lambda_2^2}{8}-\frac{u}{3}\right)\right]\ . \tag{C.4}$$

One sees from (C.3) that λ has poles at $(x = \frac{\Lambda_2^2}{8}, y = \pm i\Lambda_2^2(m_1-m_2)/8)$ with residues $\pm\frac{1}{2\pi i}\frac{m_1-m_2}{2\sqrt{2}}$ and at $(x = -\frac{\Lambda_2^2}{8}, y = \mp i\Lambda_2^2(m_1+m_2)/8)$ with residues $\pm\frac{1}{2\pi i}\frac{m_1+m_2}{2\sqrt{2}}$ [2]. In particular, for $m_1 = m_2 = m$, there are only the poles at $(x = -\frac{\Lambda_2^2}{8}, y = \mp i\Lambda_2^2 m/4)$ with residues $\pm\frac{1}{2\pi i}\frac{m}{\sqrt{2}}$.

Three flavours: $N_f = 3$

This case is more complicated since the y^2 is no longer linear in u, see eq. (2.1), (2.2). There exist expressions for λ in the literature using a quartic curve [21] instead. Proceeding along the same lines as in [21] we can obtain λ also for the cubic curve (2.1), (2.2): we write

$$\begin{aligned}y^2 = G(x) - F^2(x) \quad , \quad F(x) &= \sqrt{a}\left(x - u - \frac{x^2}{2a} + \frac{b^2}{2a}\right)\\ G(x) &= \frac{x^4}{4a} - \frac{b^2x^2}{2a} + \frac{b^4}{4a} + cx - d\end{aligned} \tag{C.5}$$

where we have set $a = \frac{\Lambda_3^2}{64}$, $b^2 = a\sum m_i^2$, $c = \frac{1}{4}\Lambda_3\prod m_i$ and $d = a\sum_{i<j} m_i^2 m_j^2$. One can then check that the following differential indeed satisfies (2.4)

$$\lambda = -\frac{\sqrt{2}}{8\pi}\frac{x\,\mathrm{d}x}{\sqrt{a}\,y}\left(\frac{F(x)G'(x)}{2G(x)} - F'(x)\right)\ . \tag{C.6}$$

In general, to express $\int\lambda$ in terms of the three elliptic integrals I_i one needs to decompose the quartic polynomial $G(x)$ into linear factors. While this can be done in general, it is cumbersome and the result not very illuminating. Here we will restrict ourselves to the simpler case $m_1 = m_2 = 0$, $m_3 \equiv m$. Then, since $c = d = 0$: $G(x) = \frac{1}{4a}(x^2-b^2)^2$ and $\frac{G'}{2G} = \frac{1}{x+b} + \frac{1}{x-b}$

where now $b = \Lambda_3 m/8$. It is then easy to see that

$$\lambda = -\frac{\sqrt{2}}{8\pi}\frac{\mathrm{d}x}{y}\left[x - 2u + \frac{b^2+bu}{x+b} + \frac{b^2-bu}{x-b}\right] \tag{C.7}$$

so that after introducing $\eta = 2y$ and $\xi = x - \frac{u}{3} - \frac{\Lambda_3^2}{192}$ we get

$$\begin{aligned}\int \lambda = \frac{\sqrt{2}}{4\pi}\Bigg[\left(\frac{5}{3}u - \frac{\Lambda_3^2}{192}\right)I_1 - I_2 - \frac{\Lambda_3 m}{64}(8u+\Lambda_3 m)I_3\left(-\frac{\Lambda_3 m}{8} - \frac{\Lambda_3^2}{192} - \frac{u}{3}\right) \\ + \frac{\Lambda_3 m}{64}(8u-\Lambda_3 m)I_3\left(\frac{\Lambda_3 m}{8} - \frac{\Lambda_3^2}{192} - \frac{u}{3}\right)\Bigg] .\end{aligned} \tag{C.8}$$

We see from (C.7) that λ has poles at $(x = \Lambda_3 m/8\,,\ y = \mp i(\Lambda_3 m/8 - u)\Lambda_3/8)$ and at $(x = -\Lambda_3 m/8\,,\ y = \pm i(-\Lambda_3 m/8 - u)\Lambda_3/8)$ with residues $\pm\frac{1}{2\pi i}\frac{m}{2\sqrt{2}}$. Note that the integrals I_3 cancel in the $m \to 0$ limit.

The pure gauge theory: $N_f = 0$

Finally let us note that for the pure gauge theory in the conventions of [2] we have

$$\int \lambda = \frac{\sqrt{2}}{4\pi}\left[uI_1 - 3I_2 - \frac{\Lambda_0^4}{4}I_3\left(-\frac{u}{3}\right)\right] . \tag{C.9}$$

Since $-\frac{u}{3}$ is one of the roots e_i one can use relations (B.11) to (B.13) to reexpress $I_3\left(-\frac{u}{3}\right)$ as a combination of I_1 and I_2. This must be so for $N_f = 0$ since λ has no poles and thus its integral must be expressible through I_1 and I_2 only.

RG flows of the integrals

One can check the different RG flows at the level of the period integrals. For example, starting with the $N_f = 1$ periods (C.2) and letting $m \to \infty$, $\Lambda_1 \to 0$ while keeping $m\Lambda_1^3 = \Lambda_0^4$ fixed, we immediately find that (C.2) flows to (C.9). The flow from $N_f = 2$, eq. (C.4), to $N_f = 1$, eq. (C.2), as $m_2 \to \infty$, $\Lambda_2 \to 0$, $m_2\Lambda_2^2 = \Lambda_1^3$ fixed, is less trivial: starting with (C.4) we have

$$\begin{aligned}\int \lambda\Big|_{N_f=2} \ \to\ \frac{\sqrt{2}}{4\pi}\Bigg[\frac{4}{3}uI_1 - 2I_2 + \frac{\Lambda_1^3}{8}(m_2-2m_1)I_3\left(-\frac{u}{3} + \frac{\Lambda_1^3}{8m_2}\right) \\ - \frac{\Lambda_1^3}{8}(m_2+2m_1)I_3\left(-\frac{u}{3} - \frac{\Lambda_1^3}{8m_2}\right)\Bigg] .\end{aligned} \tag{C.10}$$

Here, the integrals I_i on the r.h.s. are meant to be those of $N_f = 1$. Taylor expanding $I_3(c+\delta c) = I_3(c) + I_3'(c)\delta c + \ldots$, and using the relation (B.17) for the derivative of I_3 (valid for $N_f = 1$), the r.h.s of eq. (C.10) becomes exactly the r.h.s. of eq. (C.2), up to terms that vanish as $m_2 \to \infty$. Similarly one can check that as $m \to \infty$, the $N_f = 3$ periods (C.8) flow to the $N_f = 2$ periods (C.4) with $m_1 = m_2 = 0$. This requires to reexpress $I_3(c)$ for c a root e_i in terms of I_1 and I_2 through the formulae given in appendix B.

APPENDIX D

In this appendix we perform some checks on our equations (2.27) that express a and a_D for $N_f = 2$, $m_1 = m_2 = m$ in terms of the $I_i^{(j)}$ and hence of the complete elliptic integrals K, E and Π_1. In particular, we will show that one indeed recovers the correct expressions of the massless $N_f = 2$ theory [4] as $m \to 0$, and that one gets the appropriate expressions of $N_f = 0$ in the $m \to \infty$ limit.

First we examine the limit $m \to 0$. Then the extra term $\frac{m}{\sqrt{2}}$ in (2.27) disappears and one has

$$\begin{aligned}\oint_{\gamma_i} \lambda \to & \frac{\sqrt{2}}{4\pi}\left[\frac{4}{3}u\, I_1^{(i)} - 2I_2^{(i)}\right] = \frac{\sqrt{2}}{4\pi}\oint_{\gamma_i}\frac{\mathrm{d}\xi\left(\frac{4}{3}u - 2\xi\right)}{\eta} \\ = & \frac{\sqrt{2}}{4\pi}\oint_{\gamma_i}\frac{\mathrm{d}x(u-x)}{y} = -\frac{\sqrt{2}}{4\pi}\oint_{\gamma_i}\frac{\mathrm{d}x\sqrt{x-u}}{\sqrt{x^2 - \frac{\Lambda_2^4}{64}}}\,.\end{aligned} \tag{D.1}$$

Since $e_1 \to \frac{2u}{3}$, $e_2 \to -\frac{u}{3} + \frac{\Lambda_2^2}{8}$, $e_3 \to -\frac{u}{3} - \frac{\Lambda_2^2}{8}$ (or in terms of the variable x the roots are $x_1 = u$, $x_2 = \frac{\Lambda_2^2}{8}$), these are precisely the integral expressions for a_D and a of the massless $N_f = 2$ theory (which equal $\frac{1}{2}$ times the a_D and a of the $N_f = 0$ theory) [1, 4].

Now let $m \neq 0$. It is then straightforward to explicitly check that at the rightmost singularity, $u = m^2 + \frac{\Lambda_2^2}{8}$, we have the following: if $m < \frac{\Lambda_2}{2}$ one has $e_1 = e_2$, $k' = 0$ and thus it follows that $a_D(u) = 0$; if $m > \frac{\Lambda_2}{2}$, however, one has $e_2 = e_3$ so that $k = 0$ and it then follows that $a(u) = \frac{m}{\sqrt{2}}$. Hence we see that the massless BPS state at this singularity $u = m^2 + \frac{\Lambda_2^2}{8}$ is a magnetic monopole $(n_e, n_m)_s = (0,1)_0$ if $m < \frac{\Lambda_2}{2}$, while for $m > \frac{\Lambda_2}{2}$ it is a quark $(n_e, n_m)_s = (1,0)_1$. This perfectly agrees with the discussion of Section 2 and thus justifies the choice of adding the $\frac{m}{\sqrt{2}}$ term in the first equation (2.27).

Let us now examine the RG flow to the $N_f = 0$ theory as $m \to \infty$, $\Lambda_2 \to 0$, $m\Lambda_2 = \Lambda_0^2$ fixed. The flow of the roots e_i of eq. (A.9) is

$$\begin{aligned} e_1 &\to \frac{u}{6} + \frac{1}{2}\sqrt{u+\Lambda_0^2}\sqrt{u-\Lambda_0^2} \equiv e_1^{(0)} \\ e_2 &\to -\frac{u}{3} \equiv e_3^{(0)} \\ e_3 &\to \frac{u}{6} - \frac{1}{2}\sqrt{u+\Lambda_0^2}\sqrt{u-\Lambda_0^2} \equiv e_2^{(0)}\,. \end{aligned} \tag{D.2}$$

where $e_i^{(0)}$ is the standard labeling of the roots for $N_f = 0$. We see that the flow exchanges the labelling of e_2 and e_3. Let us first consider the flow of $a(u)$ as given by the first eq. (2.27). Since the $N_f = 2$ curve flows to the $N_f = 0$ curve, the integrands flow appropriately. Clearly, the cycle $\gamma_1^{(N_f=2)}$ encircling e_2 and e_3 flows to the cycle $\gamma_1^{(N_f=0)}$. Hence $I_1^{(1)} \to I_1^{(1)}|_{N_f=0}$ and $I_2^{(1)} \to I_2^{(1)}|_{N_f=0}$. The integral $I_3^{(1)}$ is more subtle since it is the one that involves the pole at

$c = -\frac{u}{3} - \frac{\Lambda_2^2}{8} = e_3^{(0)} - \frac{\Lambda_2^2}{8}$. As $\Lambda_2 \to 0$, this pole approaches $e_3^{(0)}$. Hence, for non-zero $\frac{\Lambda_2^2}{8}$ the pole at $\xi = c$ is outside the integration contour. As $\Lambda_2 \to 0$, the pole crosses the contour and $I_3^{(1)}$ picks up a contribution from the residue which is $\delta I_3^{(1)} = \frac{4\pi}{\Lambda_2^2 m}$ which precisely cancels the additional term $\frac{m}{\sqrt{2}}$ in eq. (2.27). Hence

$$a(u) \to \frac{\sqrt{2}}{4\pi}\left[\frac{4}{3}\,u I_1^{(1)} - 2\,I_2^{(1)} - \frac{\Lambda_0^4}{2}\,I_3^{(1)}(e_3^{(0)})\right]\Bigg|_{N_f=0} . \tag{D.3}$$

Using the relation $I_3^{(1)}(e_3^{(0)})\Big|_{N_f=0} = \frac{4}{\Lambda_0^4}\left(I_2^{(1)} + \frac{u}{3}\,I_1^{(1)}\right)\Big|_{N_f=0}$ from appendix B, we see that the r.h.s. of eq. (D.3) indeed coincides with the corresponding integral for $N_f = 0$, and hence $a(u) \to a(u)\Big|_{N_f=0} \equiv a^{(0)}(u)$. Next, let us discuss the flow of $a_D(u)$. The cycle γ_2 encircles e_1 and e_2 which flow to $e_1^{(0)}$ and $e_3^{(0)}$. The corresponding integral thus is the sum of the integral over a cycle $\gamma_2^{(0)}$ around $e_1^{(0)}$ and $e_2^{(0)}$ and one over a cycle $\gamma_1^{(0)}$ around $e_2^{(0)}$ and $e_3^{(0)}$: $\gamma_2 \to \gamma_2^{(0)} + \epsilon\gamma_1^{(0)}$ where $\epsilon = \mathrm{sign}(\Im m\, u)$. Again, the pole crossing the cycle $\gamma_1^{(0)}$ gives a term $-\epsilon\frac{m}{\sqrt{2}}$. As a result we have

$$\begin{aligned} a(u) &\to a^{(0)}(u) \\ a_D(u) + \epsilon\,\frac{m}{\sqrt{2}} &\to a_D^{(0)}(u) + \epsilon\, a^{(0)}(u)\ . \end{aligned} \tag{D.4}$$

This motivates us to define $\tilde{a}_D(u) = a_D(u) - \epsilon\left(a(u) - \frac{m}{\sqrt{2}}\right)$ which is such that under the RG flow as $m \to \infty$ one has $\tilde{a}(u) \to a^{(0)}(u)$ and $\tilde{a}_D(u) \to a_D^{(0)}(u)$.

Acknowledgements:

We are grateful to E. Brézin for an interesting discussion, as well as to I. Bakas for pointing out to us some properties of the elliptic integral of the third kind.

REFERENCES

1. N. Seiberg and E. Witten, *Electric-magnetic duality, monopole condensation, and confinement in $N = 2$ supersymmetric Yang-Mills theory*, Nucl. Phys. **B426** (1994) 19, hep-th/9407087.
2. N. Seiberg and E. Witten, *Monopoles, duality and chiral symmetry breaking in $N = 2$ supersymmetric QCD*, Nucl. Phys. **B431** (1994) 484, hep-th/9408099.
3. F. Ferrari and A. Bilal, *The strong-coupling spectrum of Seiberg-Witten theory*, Nucl. Phys. **B469** (1996) 387, hep-th/9602082.
4. A. Bilal and F. Ferrari, *Curves of marginal stability, and weak and strong coupling BPS spectra in N=2 supersymmetric QCD*, Nucl. Phys. **B480** (1996) 589, hep-th/9605101.
5. A. Bilal, *Discontinuous BPS spectra in $N = 2$ susy QCD*, Nucl. Phys. B (Proc. Suppl.) **52A** (1997) 305-313, hep-th/9606192.
6. P.C. Argyres and M.R. Douglas, *New phenomena in* SU(3) *supersymmetric gauge theory*, Nucl. Phys. **B448** (1995) 93,hep-th/9505062.
7. P.C. Argyres, M.R. Plesser, N. Seiberg and E. Witten, *New $N = 2$ superconformal field theories in four dimensions*, Nucl. Phys. **B461** (1996) 71, hep-th/9511154.
8. F. Ferrari, *Charge fractionisation in $N = 2$ supersymmetric QCD*, Phys. Rev. Lett. **78** (1997) 795, hep-th/9609101.
9. A. Brandhuber and S. Stieberger, *Self-dual strings and stability of BPS states in $N = 2$* SU(2) *gauge theories*, Nucl. Phys. **B488** (1997) 199, hep-th/9610053.
10. A. Klemm, W. Lerche, P. Mayr, C. Vafa and N. Warner, *Self-dual strings and N=2 supersymmetric field theory*, Nucl. Phys. **B477** (1996) 746, hep-th/9604034;
    J. Schulze and N.P. Warner, *BPS geodesics in N=2 supersymmetric Yang-Mills theory*, hep-th/9702012;
    J. Rabin, *Geodesics and BPS states in N=2 supersymmetric QCD*, hep-th/9703145.
11. F. Ferrari, *The dyon spectra of finite gauge theories*, LPTENS preprint 96/67, to appear in Nucl. Phys. B, hep-th/9702166.
12. L. Alvarez-Gaumé, M. Marino, F. Zamora, *Softly broken N=2 QCD with massive quark hypermultiplets (I)*, hep-th/9703072.
13. H. Aoyama, T. Harano, M. Sato and S. Wada, *Multi-instanton calculus in $N = 2$ supersymmetric QCD*, Phys. Lett. **B388** (1996) 331,hep-th/9607076
    T. Harano and M. Sato, *Multi-instanton calculus versus exact results in $N = 2$ supersymmetric QCD*, hep-th/9608060.
14. A. Erdelyi et al, *Higher Transcendental Functions*, Vol 1, McGraw-Hill, New York, 1953.
15. G. Mack, *All unitary ray representations of the conformal group* SU(2,2) *with positive energy*, Comm. Math. Phys. **55** (1977) 1.
16. T. Eguchi, K. Hori, K. Ito and S.K. Yang, *Study of $N = 2$ superconformal field theories in 4 dimensions*, Nucl. Phys. **B471** (1996) 430, hep-th/9603002.

17. P.C. Argyres, *S-duality and global symmetries in $N = 2$ supersymmetric field theory*, `hep-th/9706095`.

18. M. Douglas and S. Shenker, *Dynamics of* SU(n) *supersymmetric gauge theory*, Nucl. Phys. **B447** (1995) 271.

19. E.T. Whittaker and G.N. Watson, *A course of modern analysis*, Cambridge University Press (1963).

20. K. Chandrasekhara, *Elliptic functions*, Springer-Verlag (Berlin, 1985).

21. Yuji Ohta, *Prepotentials of $N = 2$ $SU(2)$ Yang-Mills theories coupled with massive matter multiplets*, J. Math. Phys. **38** (1997) 682, `hep-th/9604059`.

22. J.L. Cardy, Nucl. Phys. **B170** (1980) 369and Nucl. Phys. **B205** (1982) 17.